Atmospheric
Chemistry
and Physics
Discussions

Open Access

Volatility basis-set approach simulation of organic aerosol formation in East Asia: implications for anthropogenic-biogenic interaction and controllable amounts

H. Matsui[1], M. Koike[2], Y. Kondo[2], A. Takami[3], J. D. Fast[4], Y. Kanaya[1], and M. Takigawa[1]

[1]Research Institute for Global Change, Japan Agency for Marine-Earth Science and Technology, Kanagawa, Japan
[2]Department of Earth and Planetary Science, Graduate School of Science, University of Tokyo, Tokyo, Japan
[3]National Institute for Environmental Studies, Ibaraki, Japan
[4]Pacific Northwest National Laboratory, Richland, Washington, USA

Correspondence to: H. Matsui (matsui@jamstec.go.jp)

ACPD

14, 6203–6260, 2014

VBS OA Simulation in East Asia

H. Matsui et al.

Title Page

Abstract	Introduction
Conclusions	References
Tables	Figures

Back | Close

Full Screen / Esc

Printer-friendly Version

Interactive Discussion

Abstract

Organic aerosol (OA) simulations using the volatility basis-set approach were made for East Asia and its outflow region. Model simulations were evaluated through comparisons with OA measured by aerosol mass spectrometers in and around Tokyo (at Komaba and Kisai in summer 2003 and 2004) and over the outflow region in East Asia (at Fukue and Hedo in spring 2009). The simulations with aging processes of organic vapors reasonably well reproduced mass concentrations, temporal variations, and formation efficiency of observed OA at all sites. As OA mass was severely underestimated in the simulations without the aging processes, the oxidations of organic vapors are essential for reasonable OA simulations over East Asia. By considering the aging processes, simulated OA concentrations increased from 0.24 to 1.28 μg m^{-3} in the boundary layer over the whole of East Asia. OA formed from the interaction of anthropogenic and biogenic sources was also enhanced by the aging processes. The fraction of controllable OA was estimated to be 87 % of total OA over the whole of East Asia, showing that most of the OA in our simulations formed anthropogenically (controllable). Even a large portion of biogenic secondary OA (78 % of biogenic secondary OA) was formed through the influence of anthropogenic sources. The high fraction of controllable OA in our simulations is likely because anthropogenic emissions are dominant over East Asia and OA formation is enhanced by anthropogenic sources and their aging processes. Both the amounts (from 0.18 to 1.12 μg m^{-3}) and the fraction (from 75 % to 87 %) of controllable OA were increased by aging processes of organic vapors over East Asia.

1 Introduction

Organic aerosol (OA) accounts for a significant mass fraction of the submicron aerosols in the atmosphere (Kanakidou et al., 2005; Zhang et al., 2007), and it influences the Earth's climate both directly (by scattering/absorbing of solar radiation) and indirectly

(by modifying cloud microphysical properties) (Hallquist et al., 2009). OA is directly emitted from fossil fuel combustion, biomass burning, and other sources (primary organic aerosol, POA) or formed through the oxidation of thousands of volatile organic compounds (VOCs) in the atmosphere (secondary organic aerosol, SOA). Recent studies show that SOA accounts for a large fraction of OA globally (e.g., Kanakidou et al., 2005; Goldstein and Galbally, 2007; Zhang et al., 2007; de Gouw and Jimenez, 2009; Hallquist et al., 2009; Pye and Seinfeld, 2010; Heald et al., 2011; Jathar et al., 2011; Spracklen et al., 2011). However, as SOA formation processes are very complicated, estimates of the SOA burden in the atmosphere and its impact on climate and human health remain highly uncertain compared with those of other aerosols such as inorganic species (Hallquist et al., 2009). The current estimation of global SOA formation rate is about 30–450 Tg yr^{-1} (Hallquist et al., 2009; Heald et al., 2010; Farina et al., 2010; Spracklen et al., 2011; Lin et al., 2012).

In the traditional OA models, the mass concentrations of SOA produced from individual parent VOCs (isoprene and terpenes for biogenic VOCs, and benzene, toluene and xylene for anthropogenic VOCs) are calculated with two mass-based yield coefficients and two partitioning coefficients which are estimated by fitting of laboratory experimental results (two-product approach) (Odum et al., 1996, 1997). Using this approach, various global- and regional-scale simulations have been made (e.g., Andersson-Sköld and Simpson, 2001; Chung and Seinfeld, 2002; Tsigaridis and Kanakidou, 2003, 2005, 2007; Heald et al., 2005, 2008; Liao and Seinfeld, 2005; Tsigaridis et al., 2006; Henze et al., 2008; Hoyle et al., 2009; O'Donell et al., 2011), but they have underestimated observed OA and/or SOA concentrations and formation rates in the atmosphere by approximately an order of magnitude, especially over urban regions (e.g., McKeen et al., 2007; Han et al., 2008; Matsui et al., 2009a).

More recently, a significant source of SOA was proposed by laboratory studies (e.g., Robinson et al., 2007), which found missing sources of semivolatile and intermediate organic compounds (SIVOCs) and the importance of chemical aging of SIVOCs and VOCs in the atmosphere. Donahue et al. (2006) developed a new framework for OA

modeling, the volatility basis set (VBS) approach. In the VBS, individual organic vapors are categorized to surrogate species with similar volatility, and their photochemical multigenerational oxidation and gas/particle partitioning processes are calculated. The VBS approach has recently been applied to both global- and regional-scale simula-
5 tions (e.g., Lane et al., 2008a, b; Farina et al., 2010; Pye and Seinfeld, 2010; Pye et al., 2010; Jathar et al., 2011; Athanasopoulou et al., 2013). Improvement of the agreement between oxygenated OA (OOA, a measure of SOA) observed by aerosol mass spectrometers (AMS) and simulated SOA was reported for the air over Mexico City (Hodzic et al., 2010; Tsimpidi et al., 2010, 2011; Li et al., 2011; Shrivastava et al., 2011), the
10 United States (Ahmadov et al., 2012), and Europe (Fountoukis et al., 2011; Bergström et al., 2012; Athanasopoulou et al., 2013; Zhang et al., 2013).

    East and Southeast Asia is one of the largest sources of aerosols in the world (e.g., Streets et al., 2003; Dentener et al., 2006; Zhang et al., 2009; Bond et al., 2013). Many studies have reported impacts of Asian aerosols on regional and hemispherical scales
15 (e.g., Ramanathan et al., 2001; Carmichael et al., 2003; Tang et al., 2003, 2004; Nakajima et al., 2007; Liu et al., 2008; Adhikary et al., 2010; Matsui et al., 2011a, b, 2013a; Oshima et al., 2012, 2013). Several global and regional modeling studies have simulated and evaluated OA over East Asia (e.g., Heald et al., 2005, 2011; Han et al., 2008; Dunlea et al., 2009; Matsui et al., 2009a; Utembe et al., 2011; Jiang et al., 2012; Lin
20 et al., 2012; Li et al., 2013; Mahmud and Barsanti, 2013). Most of previous OA simulation studies underestimated observed OA and SOA concentrations over the region. For example, Utembe et al. (2011) evaluated their global OA simulations over the outflow region in East Asia through the comparisons with OA measurements during the ACE-Asia campaign. While their simulations reproduced the vertical profile of observed OA
25 mass concentrations, they underestimated absolute OA mass concentrations by a factor 5. Matsui et al. (2009a) made OA simulations over Tokyo urban area in July and August 2003. The simulations reproduced absolute concentrations and their temporal variations of observed NO_x, ozone (O_3), VOCs, and inorganic aerosols reasonably well,

but severely underestimated observed SOA (by a factor of 5) and OA concentrations (by a factor of 2).

Few studies have focused on OA concentrations and their spatial distributions over the whole of East and Southeast Asia and its outflow region (Han et al., 2008; Jiang et al., 2012). They also underestimated observed OA and/or SOA concentrations over China. To our knowledge, the VBS approach with the oxidation processes of organic vapors has not been applied and evaluated to study OA concentrations and their spatial distributions over the Asian region. As the VBS approach has a potential to explain realistic OA concentrations over East and Southeast Asia, the application and evaluation of the VBS approach to the Asian region is important for more quantitative understanding of OA concentrations and their spatial distributions over the region.

The understanding on the interaction of anthropogenic and biogenic sources is also very limited over the Asian region. Anthropogenic sources may substantially influence biogenic SOA (BSOA) formation (e.g., Carlton et al., 2010; Hoyle et al., 2011; Spracklen et al., 2011). The formation of BSOA is enhanced by anthropogenic POA, NO_x, and VOCs because they increase the concentrations of precursor VOCs, the oxidation rates of VOCs, and the particle-to-gas partitioning ratios of organic compounds (e.g., Heald et al., 2008; Tsigaridis et al., 2006; Tsigaridis and Kanakidou, 2007). Carlton et al. (2010) estimated the effect of anthropogenic emissions on BSOA formation and demonstrated that more than 50 % of predicted BSOA concentrations were influenced by anthropogenic emissions in the eastern United States. Some global modeling studies estimated much higher contributions from enhanced BSOA (Tsigaridis et al., 2006; Hoyle et al., 2009; Spracklen et al., 2011). As both anthropogenic and biogenic emissions are very large over East and Southeast Asia, the interaction of anthropogenic and biogenic sources and the resulting enhancement of BSOA is very important and should be examined for the region. These understandings would be useful to estimate the past, current, and future OA concentrations and their regional and hemispherical climatic impacts.

The objective of this study is to understand OA concentrations and their spatial distributions over all of East and Southeast Asia and its outflow region with the interaction of anthropogenic and biogenic sources. We simulated OA concentrations over East Asia and its outflow region by using a VBS model we developed (Sect. 2), and evaluated the results through comparisons with AMS measurements conducted in and around Tokyo and over the outflow region in East Asia (Sects. 3 and 4). OA spatial distributions over East Asia are described with the importance of aging treatments in the VBS (Sect. 5.1.1). We also examined the interaction of anthropogenic and biogenic sources in OA formation processes, such as the enhancement of BSOA formation due to aging processes of anthropogenic SIVOCs and VOCs (Sect. 5.1.2). Finally, we estimated the contribution of anthropogenically induced (controllable) OA over East Asia and the impact of aging treatments on it (Sect. 5.2). The abbreviations of organic vapors and aerosols used in this study are summarized in Table 1.

2 Regional three-dimensional model

2.1 WRF-chem model

In this study, we used the Weather Research and Forecasting/Chemistry (WRF-chem) model with the MOSAIC aerosol module (version 3.4) (Skamarock et al., 2008; Grell et al., 2005; Fast et al., 2006; Zaveri et al., 2008), which has been used in our previous studies (Matsui et al., 2009b, 2010, 2011c, 2013b, c), with modifications of the schemes related to organic aerosol formation (see Sect. 2.2). The chemical processes considered in the original WRF-chem model are emissions of gaseous and aerosol species, gas-phase chemistry (Zaveri and Peters, 1999), new particle formation (Wexler et al., 1994), dynamical gas-particle partitioning (condensation/evaporation) (Zaveri et al., 2005a, b, 2008), Brownian coagulation (Jacobson et al., 1994), aqueous-phase chemistry (Fahey and Pandis, 2001), and dry and wet deposition (Easter et al., 2004). The mass (sulfate, nitrate, ammonium, black carbon, POA, dust, sodium, chloride, and

aerosol water) and number concentrations of aerosol are explicitly calculated for the size range from 40 nm to 10 µm in 8 size bins. The meteorological and chemical process options adopted in this study are summarized in Table 2. More detailed descriptions of the WRF-chem/MOSAIC model are given elsewhere (Fast et al., 2006).

2.2 OA formation scheme (VBS)

The WRF-chem model was modified to consider OA formation processes using the VBS approach (Fig. 1). Table 3 shows the summary of the OA formation scheme developed in this study. Similar to previous studies (e.g., Lane et al., 2008a; Tsimpidi et al., 2010; Shrivastava et al., 2011), this study used 9 surrogate volatility species to represent SIVOCs with effective saturation concentrations (C^*, saturation concentrations at 300 K) of 10^{-2}, 10^{-1}, 1, 10, 10^2, 10^3, 10^4, 10^5, and 10^6 µg m^{-3}. Gas-phase chemistry was represented by the SAPRC99 mechanism (Carter, 2000) with the formation of first-generation oxidized VOCs (OVOCs) from the 9 lumped VOCs; alkanes (ALK4 and ALK5), olefins (OLE1 and OLE2), aromatics (ARO1 and ARO2), isoprene (ISOP), monoterpene (TERP), and sesquiterpene (SESQ). The mass yield of OVOCs from each lumped VOC was calculated with the same NO$_x$-dependent 4-product basis fit (C^* of 1, 10, 100, and 1000 µg m^{-3}) used in Tsimpidi et al. (2010). SIVOCs and OVOCs were oxidized to the surrogate species with an order of magnitude lower C^* by OH radical with an assumed rate constant of 1×10^{-11} cm^3 molecule^{-1} s^{-1} (Fig. 1). The increase in SOA mass due to the addition of an oxygen atom was taken into account, as described by Tsimpidi et al. (2010): 7.5 % increase for the reduction of volatility by one order of magnitude. The enthalpy of vaporization was based on Tsimipidi et al. (2010) and Lane et al. (2008a): 64–112 kJ mol^{-1} for POA and 30 kJ mol^{-1} for SOA. Our scheme traced 53 surrogate vapor species (9 for primary SIVOCs, 8 for oxygenated SIVOCs, and 36 for OVOCs) and the corresponding 53 aerosol species for bulk aerosol mass concentrations. In this study, we defined oxidized POA (OPOA) as OA from oxygenated SIVOCs, anthropogenic SOA (ASOA) as OA from anthropogenic

VOCs (ALK4, ALK5, OLE1, OLE2, ARO1, and ARO2), and biogenic SOA (BSOA) as OA from biogenic VOCs (ISOP, TERP, and SESQ) (Fig. 1).

The scheme assumes equilibrium between the vapor and particulate species. Bulk equilibrium gas-particle partitioning was calculated with an iteration scheme of Schell et al. (2001). The changes in size-resolved mass concentrations in 8 size bins were calculated based on Koo et al. (2003) with the Kelvin effect. The fraction of total flux of species i between gas and aerosol phases that condenses onto or evaporates from aerosol size bin k ($f_{i,k}$) is given by

$$f_{i,k} = \frac{2\pi N_k d_k D_i F \left(C_i - C_i^{\text{eq}} \eta\right)}{\sum_k 2\pi N_k d_k D_i F \left(C_i - C_i^{\text{eq}} \eta\right)} \tag{1}$$

where N_k is the number concentrations in bin k, d_k is the mean diameter of bin k, D_i, C_i, and C_i^{eq} are the diffusivity, bulk gas-phase concentration, and equilibrium concentration at the particle surface of species i, respectively, F is the correction for non-continuum effects which depends on the Knudsen number and the accommodation coefficient (0.1 was assumed), and η is the Kelvin effect correction. In our scheme, Eq. (1) was calculated for individual VBS species (53 species), but all of the size-resolved information was not directly used for the calculation of three-dimensional transport processes to reduce computational cost. Only total OA (sum of all VBS species) was transported with the size-resolved information, and individual VBS species were transported with the information of bulk mass concentrations only (not size-resolved, we assumed all VBS species had the same size distribution). This treatment can reduce the number of transport variables (therefore computational cost) by a factor of 4 compared with the size-resolved treatment for all VBS species and by a factor of 3 compared with the 4-bin scheme in Shrivastava et al. (2011) which is implemented in original WRF-chem model (Table 3). Therefore, the scheme developed in this study is a detailed (9 species), size-resolved (for total OA), and computationally efficient VBS scheme.

The emission factors of SIVOCs/POA were assumed based on Shrivastava et al. (2011). In this study, we applied the factors for anthropogenic sources (Table 2 of Shrivastava et al., 2011) to all the emission sources. The sum of all SIVOCs/POA emissions is 7.5 times traditional POA emissions (Fig. 1), which is based on the rough esti-
5   mate of the SVOC/POA ratio of 3 and the IVOC/SVOC ratio of 1.5 (or the IVOC/POA ratio of 4.5) in previous studies (Tsimpidi et al., 2010; Shrivastava et al., 2011). To make consistent aerosol number concentrations between traditional OA emissions and SIVOCs/POA emissions, we assumed particulate emissions (POA) for C^* ranging from 10^{-2} to $1\,\mu g\,m^{-3}$, gas-phase emissions (SIVOCs) for C^* ranging from 10^6 to $10^2\,\mu g\,m^{-3}$,
10   and the mixture of gas-phase and particulate emissions for C^* of $10\,\mu g\,m^{-3}$ (Fig. 1).

Dry deposition of organic vapors (SIVOCs and OVOCs) was calculated by the scheme of Wesely (1989), which was used in the original WRF-chem/MOSAIC model. In this study, the dry deposition velocity of HNO_3 was assumed for all the organic vapors, which is consistent with Ahmadov et al. (2012). OA concentrations are sensitive
15   to this assumption because a factor of 2 different velocities led to an increase/decrease in OA concentrations about 50 % in our application over East Asia. Dry deposition of OA was calculated for each size bin with the scheme used in the original WRF-chem model (Binkowski and Shankar, 1995; Easter et al., 2004). Wet deposition of organic vapors (below cloud scavenging by rain) was calculated by assuming the mass transfer
20   rate of HNO_3 to rain given in Levine and Schwarz (1982). Wet deposition of OA was calculated for each size bin for in-cloud and below-cloud scavenging as calculated in the original WRF-chem model (Easter et al., 2004). A hygroscopicity value (κ) of 0.14, which was the value used in the original WRF-chem for POA, was assumed for all the OA species used in the VBS.

25   In our VBS model, oxidation processes are considered only for gaseous species, namely, homogenous aging by OH radical. Our model did not consider other processes, such as aqueous-phase reactions (e.g., Ervens et al., 2008, 2010, 2011; Lim et al., 2010; Liu et al., 2012), heterogeneous oxidation (e.g., George et al., 2007, 2008), oligomerization (e.g., Kalberer et al., 2004; Iinuma et al., 2004), and fragmentation

VBS OA Simulation in East Asia

H. Matsui et al.

Title Page

Abstract	Introduction
Conclusions	References
Tables	Figures

|◀ | ▶|

◀ | ▶

Back | Close

Full Screen / Esc

Printer-friendly Version

Interactive Discussion

(e.g., Jimenez et al., 2009; Kroll et al., 2009; Murphy et al., 2012). These processes could be important because they alter volatility and oxidation state (i.e., an atomic O/C ratio) of organic vapors and OA, leading to changes in OA concentrations. However, currently these processes have large uncertainties in reaction rates and products (Hallquist et al., 2009). Some recent studies developed two-dimensional VBS schemes (2D-VBS), in which both volatility and oxidation state were calculated considering functionalization and fragmentation (e.g., Jimenez et al., 2009; Donahue et al., 2011; Murphy et al., 2011, 2012; Shrivastava et al., 2013). In Murphy et al. (2012), heterogeneous oxidation and aqueous-phase chemistry processes are also taken into account. They applied their one-dimensional (column) chemical transport model to Europe and showed that the simple one-dimensional (volatility only) VBS (1D-VBS) scheme reproduced observed OA mass concentrations and O/C ratios reasonably well and that the performance of the 1D-VBS scheme was not worse than that of their more complex 2D-VBS schemes, likely due to uncertainties in the understanding of SOA evolution in the atmosphere. Considering these uncertainties and computational costs of complex VBS schemes, we used a simpler VBS scheme in this study.

Our VBS scheme also has also large uncertainties in the treatment of aging parameters, emission factors, and dry and wet deposition of organic vapors, which could change simulated OA concentrations considerably. In this study, we examined the sensitivity of aging coefficients (Sect. 4.3, Table 2). Other uncertainties are not discussed in this paper. The uncertainties in emission factors and the treatment of dry deposition for organic vapors used in the VBS scheme are described by Tsimpidi et al. (2010) and Ahmadov et al. (2012).

3   Measurements and simulation setups

In this study, we simulated OA formation both in and around Tokyo urban area (Sect. 2.3.1) and over East Asia (Sect. 2.3.2). The purpose of the simulation in and around Tokyo is to validate the VBS scheme over the region where meteorological

fields, emissions, and the concentrations of precursor gaseous species are relatively well known (compared with over the Asian region). We can use observed data during the Integrated Measurement Program for Aerosol and oxidant Chemistry in Tokyo (IM-PACT) campaign (Takegawa et al., 2006a, b; Kondo et al., 2006, 2007, 2008, 2010).

5 OA mass concentrations observed with an Aerodyne AMS and gaseous species such as O_3, OH, and VOCs are available for the campaign period. These observation data can be used not only to validate the simulations but also to constrain the parameters related to OA formation such as precursor VOCs. The simulation over Asia was conducted to understand the behavior of OA over all of East and Southeast Asia and its

10 outflow region, though there are uncertainties in emissions and limitations of validations especially for precursor gases. OA mass concentrations (Aerodyne AMS) at two sites in Japan were used to evaluate the simulations over the outflow regions from the Asian continent.

3.1 Simulation in and around Tokyo (summer 2003 and 2004)

15 We used OA mass concentrations observed by an Aerodyne AMS and gaseous species of O_3 and VOCs at an urban area, Komaba (35.66° N, 139.67° E), Tokyo, in July and August 2003 during the IMPACT-2 campaign and at a suburban site, Kisai (36.08° N, 139.55° E), Saitama, in July and August 2004 during the IMPACT-L campaign (Fig. 2a). Details of the measurements are given elsewhere (Takegawa et al.,

20 2005, 2006a, b; Kondo et al., 2006, 2007, 2008, 2010; Shirai et al., 2007; Kanaya et al., 2007).

The oxygenated and hydrocarbon-like OA concentrations (OOA and HOA) were estimated by a custom solution procedure (least-squares fits to the time series of OA) using AMS-derived signals at mass-to-charge (m/z) ratios 44 and 57 (Zhang et al., 2005).

25 Though there are some uncertainties in this method, the OOA/HOA concentrations derived from this method can be used as a proxy of SOA/POA concentrations because SOA and POA concentrations, which were estimated from the correlation of total OA with CO, correlated well with HOA and OOA with slopes of 0.88–1.36 and 0.97–1.41,

respectively, during the IMPACT campaign (Takegawa et al., 2006a, b; Kondo et al., 2007). We used observed HOA concentrations to constrain POA emissions and to simulate realistic POA concentrations by the model (see below). Observed OOA was used to validate simulated SOA (Sect. 4.1).

5   For the simulation in and around Tokyo, the horizontal grid spacings in the model domain were 27 km (outer domain) and 9 km (inner domain) (horizontal scale of $9° \times 7°$, Fig. 2a), and there were 18 vertical levels from the surface to 100 hPa. The lowest layer was about 30 m in depth. The simulation periods were 17 July–15 August 2003 during the IMPACT-2 campaign and 23 July–15 August 2004 during the IMPACT-L campaign.

10 The first 2 days of data were used for model spin-up. The National Centers for Environmental Prediction (NCEP) Final (FNL) Operational Global Analysis data were used for initial and boundary conditions and nudging (free troposphere only) of meteorological fields. We made two model simulations, with and without aging processes of organic vapors in the VBS.

15 We used anthropogenic emission inventories for 1998 at a horizontal resolution of $10 \times 10\,km^2$ with seasonal and diurnal dependencies (Kannari et al., 2004). The detailed description of the inventories is given by Matsui et al. (2009a). We also used on-line biogenic emissions: the Model of Emissions of Gases and Aerosols from Nature version 2 (MEGAN2) (Guenther et al., 2006). Using the same approach as described in

20 Matsui et al. (2009a), the emissions of aromatics (toluene and xylene) and POA were increased or decreased over all the simulation domains (without modification of spatial emission patterns) to achieve good agreement between observed and simulated mean concentrations of these species at the Komaba site during the IMPACT-2 campaign: ARO1 (toluene-like) and ARO2 (xylene-like) emissions were reduced by 50 %

25 and 30 %, respectively, and POA emissions were increased by 25 %. As the simulations with these modifications can reproduce mean concentrations of aromatics and POA during the simulation period, at least at and around Komaba, we can robustly evaluate the performance of OA formation processes.

|◀ | ▶|

◀ | ▶

Back | Close

Full Screen / Esc

Printer-friendly Version

Interactive Discussion

3.2 Simulation over East Asia (spring 2009)

We used OA and sulfate mass concentrations observed with an Aerodyne AMS at Fukue (32.75° N, 128.68° E) and Hedo (26.87° N, 128.25° E), Japan, in March and April 2009 during the Aerosol Radiative Forcing in East Asia (A-FORCE) aircraft cam-
5   paign (Oshima et al., 2012). Details of the AMS measurements at Fukue and Hedo are described by Takami et al. (2005, 2007). OA measurements over the outflow regions in East Asia are limited and they are useful to evaluate model simulations. The air parcels observed at Fukue and Hedo represent the history of sources from wide areas over northern China and their histories during the transport (e.g., Kondo et al., 2011;
10 Matsui et al., 2013a), which suggests model evaluations at these sites are suitable for overall validations of sources, transport, and transformation of aerosols from the Asian continent to the Pacific.

For the simulation over East Asia, the horizontal grid spacings for the model domain were 180 km (outer domain) and 60 km (inner domain) (horizontal scale of 120° × 60°,
15 Fig. 2b), and there were 26 vertical levels from the surface to 100 hPa. The lowest layer was about 30 m in depth. The simulation period was 21 March–26 April 2009 during the A-FORCE aircraft campaign. Statistics were calculated for 24 March–26 April 2009 period. Our previous simulations using WRF-chem successfully reproduced meteorological fields due to synoptic-scale meteorological variations and related transport and
20 variation processes of aerosol mass and number concentrations observed by both the aircraft and surface measurements during the A-FORCE period (Matsui et al., 2013b, c). The NCEP-FNL data were used for initial and boundary conditions and nudging (free troposphere only) of meteorological fields. We made 6 simulations (including the base case simulation) with different aging coefficients (Table 4).
25 We used the anthropogenic and volcanic emission inventories of Streets et al. (2003), which were also used in our previous studies (Matsui et al., 2013b, c). SO_2 emissions from the Miyakejima volcano were modified based on measurements, as shown by Matsui et al. (2013c). We also used daily biomass burning emissions from

the Global Fire Emissions Database version 3 (GFED3) (van der Werf et al., 2010), and on-line biogenic emissions from MEGAN2. On-line sea salt and dust emissions were not considered in this study.

Anthropogenic POA (from fossil fuel and biofuel combustion) was emitted mostly from China and India (Fig. 3a), while biomass burning POA was emitted mainly from Southeast Asia and Siberia (Fig. 3b). Anthropogenic and biomass burning sources account for 69 % and 31 % of total POA emissions, respectively. ARO1 (anthropogenic) emissions were distributed over China, India, Southeast Asia, Japan, and South Korea (Fig. 3c). The main source regions of TERP (biogenic) were Southeast Asia and southern China (Fig. 3d).

4   Model results and evaluation

4.1   IMPACT campaign (Tokyo)

Figure 4a and b show the time-series of O_3 and SOA at Kisai during the IMPACT-L campaign (25 July–15 August 2004). Simulated SOA is the sum of OPOA, ASOA, and BSOA. Simulated concentrations in Sect. 4 were chosen from a grid cell closest to each measurement site. Meteorological conditions during the campaign are summarized by Takegawa et al. (2006a). Northerly and easterly winds were dominant during 25–30 July, persistent southerly winds were dominant during 31 July–9 August (associated with a stable anticyclone located east of Tokyo), and the sea-land breeze circulation was dominant during 10–14 August (associated with a stable anticyclone over Tokyo). Due to these meteorological conditions, relatively fresh air was transported from the Tokyo metropolitan area to Kisai by 9 August, which was the cause of relatively low O_3 and SOA concentrations at Kisai. In contrast, stagnant and aged air was transported to Kisai during 10–14 August, which enhanced both O_3 and SOA at Kisai through the accumulation of pollutants.

VBS OA Simulation in East Asia

H. Matsui et al.

Title Page

| Abstract | Introduction |

| Conclusions | References |

| Tables | Figures |

| I◀ | ▶I |

| ◀ | ▶ |

| Back | Close |

Full Screen / Esc

Printer-friendly Version

Interactive Discussion

The simulation reproduced the absolute concentrations and the diurnal and day-to-day variations of observed O_3 and SOA concentrations reasonably well (Fig. 4 and Table 5). In particular, the model reproduced the contrast between the early (25 July–6 August, low concentrations) and the later (7–15 August, high concentrations) simula-

5 tion periods and the diurnal peak concentrations of both O_3 and SOA (Fig. 4). The daytime peak concentrations of OH and HO_2 radicals were also reproduced within 50 % at Komaba during the IMPACT-L campaign in our simulations, though the concentrations had large day-to-day variability: the median values of the daytime peak concentrations of observed OH and HO_2 were 6.3×10^6 cm^3 and 5.7 pptv, respectively (Kanaya et al.,

10 2007), and those of simulated OH and HO_2 were 9.8×10^6 cm^3 and 6.8 pptv, respectively.

As both O_3 and SOA were produced by photochemical reactions during the IMPACT-2 and IMPACT-L campaigns, the SOA/O_3 ratio can be used as an index of OA formation efficiency in a given oxidative condition (Fig. 5) (Herndon et al., 2008; Kondo et al.,

15 2008). The model simulation tends to overestimate maximum SOA concentrations during daytime and underestimate SOA concentrations during nighttime. However, mean SOA concentrations were reproduced by the model to within 25 % of the corresponding observed values (underestimation by 21 % and 13 % during the IMPACT-2 and IMPACT-L campaigns, respectively) (Table 5). In both campaigns, the simulated fitting slopes

20 (with aging processes) were also consistent with observed slopes (and hence, OA formation efficiency): observed and simulated fitting slopes were 0.16 and 0.17 during the IMPACT-2 campaign and 0.15 and 0.19, respectively, during the IMPACT-L campaign.

The simulation without aging processes (orange lines and triangles in Figs. 4 and 5), which is similar to the simulation using a traditional OA model, severely underes-

25 timated mean observed OA concentrations by 76 % and 86 % and fitting slopes by 80 % and 82 % during the IMPACT-2 and IMPACT-L campaigns, respectively. The results show that the emissions of SIVOCs and the oxidation processes of organic vapors (SIVOCs and OVOCs) must be considered for reasonable OA simulations in and around Tokyo: including these in the VBS scheme considerably improved the model's

ability to simulate OA absolute concentrations and their temporal variations in Tokyo and its outflow area at Kisai.

In our simulations, SOA was formed mainly from anthropogenic sources at Komaba and Kisai (77–80 % of total SOA). The three largest precursors of SOA were aromatics (ARO1 and ARO2, 48 %), olefins (OLE1 and OLE2, 13–18 %), and monoterpenes (TERP, 13–16 %). OPOA accounted for only 6–7 % of total SOA at both sites during the simulation periods.

4.2 A-FORCE periods (East Asia)

Figure 6a and b show the time-series of sulfate (SO_4) at the Fukue and Hedo sites during the A-FORCE campaign (24 March–26 April 2009). The meteorological conditions during this period are described by Matsui et al. (2013b, c). Synoptic-scale meteorological variations controlled temporal variations of observed aerosol concentrations at Fukue and Hedo: high concentrations during the period covered by a high-pressure system and rapid decreases in concentrations after the passage of a cold front. At Fukue, the site was covered by a high pressure system during the middle of the simulation period (6–12 April), and cold fronts passed on 14, 20, and 24 April. The temporal variations of observed SO_4 due to synoptic-scale meteorological variations were generally reproduced by the model simulation. The mean SO_4 concentrations at Fukue were also reproduced well by the model (normalized mean bias (NMB) of −11 %, Table 5), while those at Hedo were overestimated by a factor of 2 during the middle and latter parts of the simulation period (NMB of 78 %, Table 5).

Figure 6c and d shows the time-series of OA at Fukue and Hedo during the A-FORCE period. At both sites, most of the measured OA was OOA (Zhang et al., 2007) and most of the simulated OA was SOA (not shown). The temporal variations of OA were generally similar to those of SO_4 at both sites. At Fukue, the model overestimated OA concentrations during 7–15 April but underestimated them during 28 March–2 April. The model well reproduced observed OA concentrations during other periods.

Title Page

Abstract | Introduction

Conclusions | References

Tables | Figures

◄ | ►

◄ | ►

Back | Close

Full Screen / Esc

Printer-friendly Version

Interactive Discussion

The period-averaged OA concentrations were slightly overestimated (NMB of 12 %, Table 5), but the model simulations agreed well with the measurements.

At Hedo, simulated OA concentrations were overestimated by 80 % (Table 5). The period of OA overestimation corresponds to the period of SO_4 overestimation. Therefore, it is unlikely that the problems in OA formation processes only made the discrepancy between observed and simulated OA concentrations. The model likely overestimates the transport of pollutants, including precursor species and secondary aerosol formation from them.

Figure 6e and f shows the time-series of OA/SO_4 ratio at Fukue and Hedo during the A-FORCE period. The OA/SO_4 ratio was used because both OA and SO_4 at these sites are formed through oxidation processes in the atmosphere. Their oxidation pathways may not be exactly the same (OA is formed from gas-phase oxidation only, but SO_4 is formed from both gas-phase and aqueous-phase oxidation in our model), but as the formation processes of SO_4 are relatively well known compared with those of OA, the OA/SO_4 ratio can be used as an index of OA formation efficiency relative to the amounts of secondary aerosols transported to the measurement sites. The model reproduced reasonably well the period-averaged OA/SO_4 ratio observed at Fukue and Hedo: the observed ratios were 0.89 and 0.58, and the simulated ratios were 0.78 (NMB of −12 %) and 0.42 (NMB of −30 %), respectively (Table 5).

In contrast, the simulation without aging processes did not capture observed OA mass concentrations and OA/SO_4 ratios. The model without aging processes considerably underestimated both the OA concentrations (by 88 % and 83 %) and the OA/SO_4 ratio (by 85 % and 90 %) at Fukue and Hedo, respectively. The results demonstrate that the VBS scheme with aging processes much improved model performance; the scheme realistically simulated OA mass concentrations and their temporal variations and the OA/SO_4 ratio over the outflow regions in East Asia.

Simulated SOA was formed mostly from anthropogenic sources at Fukue and Hedo (90–91 % of total SOA). The three largest sources were aromatics (ARO1 and ARO2, 41–46 %), SIVOCs (34–41 %), and monoterpenes (TERP, 7–8 %). The contributions of

Title Page

Abstract	Introduction
Conclusions	References
Tables	Figures

|◄ | ►|

| ◄ | ► |

| Back | Close |

Full Screen / Esc

Printer-friendly Version

Interactive Discussion

OPOA at Fukue and Hedo (34–41 % of total SOA) were much higher than those at Komaba and Kisai (6–7 % of total SOA), due to continuous aging processes of organic vapors during transport from source areas to the measurement sites at Fukue and Hedo.

4.3 Sensitivity of aging parameters over East Asia

As shown in Sect. 2.2, the uncertainties in the aging coefficients of organic vapors are still very large in the VBS scheme. To understand the impact of these uncertainties on simulated OA mass concentrations, we conducted sensitivity simulations with the aging coefficient of $4 \times 10^{-11}\,\mathrm{cm^3\,molecule^{-1}\,s^{-1}}$ (4 times of the base case, "Aging-4") and $2.5 \times 10^{-12}\,\mathrm{cm^3\,molecule^{-1}\,s^{-1}}$ (1/4 of the base case, "Aging-0.25") (Fig. 6c and d, Table 4).

The Aging-4 (Aging-0.25) simulation increased (decreased) period-averaged OA mass concentrations by factors of 3.2 (2.1) and 4.1 (2.4) at Fukue and Hedo, respectively; thus simulated OA concentrations over East Asia were greatly affected by the choice of aging coefficients. Therefore, it is important to improve our understanding of the oxidation processes of organic vapors through laboratory and field measurements and to apply and validate the VBS scheme for various atmospheric conditions.

5 Spatial distribution of OA over East Asia

5.1 Impact of aging processes

5.1.1 Mass concentrations and contributions

Next, we examined the spatial distributions of OA over East Asia. For the simulation with the aging process, POA concentrations at an altitude of 1 km peaked over Southeast Asia and northern and central China (Fig. 7a), corresponding to large source regions of biomass burning and anthropogenic emissions, respectively (Fig. 3a and

b). ASOA concentrations were high over northern and central China and moderate over southern China, Japan, and Southeast Asia (Fig. 7c). The maximum of BSOA concentration was over Southeast Asia and southern China (Fig. 7e). Total SOA (OPOA + ASOA + BSOA) concentrations were distributed widely over East Asia with peaks over Southeast Asia and northern and central China (Fig. 7g).

The large contribution of BSOA over southern China and Southeast Asia is consistent, at least qualitatively, with previous OA modeling studies (Han et al., 2008; Jiang et al., 2012; Li et al., 2013), in which 65–90 % of SOA in southern China was estimated to be biogenic. Several measurement studies have reported mean organic carbon (OC) concentrations in spring over Guangzhou in southern China of 6–7 μg m^{-3} (Tao et al., 2012; Huang et al., 2012), over Hong Kong of 6–9 μg m^{-3} (Bahadur et al., 2009), and over Bangkok of about 10 μg m^{-3} (Sahu et al., 2011). We compared our simulation results with these measurements, though the meteorological conditions, the amounts of emissions (e.g., biomass burning, biogenic), or both may have differed between those studies and ours. When we assumed an OC-to-OA conversion rate of 1.6 (Turpin and Lim, 2001), our simulations underestimated observed OA concentrations by 35 % at Guangzou and by 60–70 % at Hong Kong and Bangkok. OOA concentrations in the Pearl River Delta region observed with an AMS have also been reported: about 5 μg m^{-3} in summer 2006 (Xiao et al., 2011) and in fall 2009 (Li et al., 2013). Our simulations underestimated the observed SOA concentrations by 30–40 % in this region. The rough comparisons shown above suggest that our OA and SOA simulations over southern China and Southeast Asia are consistent with measurements to within a factor of 3 (underestimation by 30–70 %). The agreement between measurements and model simulations over southern China and Southeast Asia was much improved by considering aging processes of organic vapors in the VBS scheme.

SOA concentrations in the Aging-off simulation were much lower than those in the Aging-on simulation (Fig. 7). By considering aging processes, ASOA, BSOA, OPOA, total SOA, and total OA concentrations over the outer domain increased between 440 % and 1380 % (Fig. 8a and Table 6), demonstrating the importance of aging processes in

OA simulations for East Asia. POA concentrations, however, varied less: the Aging-on POA concentrations over the outer domain were about 30 % more than those for the Aging-off simulations (Fig. 8a and Table 6). The lower POA concentrations in the Aging-off simulation are likely due to the smaller amounts of low-volatile organic vapors, which were produced by OH oxidation in the Aging-on simulation, and the resulting reduction of OA concentrations in the particulate phase because of the shift of gas-particle partitioning to the gas-phase.

In addition to differences in the absolute mass concentrations, the contributions from individual chemical compositions to total OA also differed greatly between the Aging-on and Aging-off simulations (Fig. 8b and c). In the Aging-on simulation, POA, OPOA, ASOA, and BSOA accounted for 18 %, 29 %, 26 %, and 27 % of OA, respectively, over the outer domain. The main precursors of ASOA were aromatics (ARO1 and ARO2, 80 % of ASOA), and those of BSOA were monoterpenes (TERP, 55 % of BSOA). In the aging-off simulation, POA was dominant (70 % of total OA) because of the formation of much less ASOA and BSOA and no OPOA.

Table 6 shows the results of the Aging-4 and Aging-0.25 simulations. Similar to the results at Fukue and Hedo (Sect. 4.3), SOA concentrations were highly sensitive to aging coefficients over the simulation domain. The period-averaged mass concentrations of OPOA, ASOA, and BSOA were enhanced (reduced) by factors of 3.3 (6.6), 2.0 (3.1), and 1.9 (2.6), respectively, in the Aging-4 (Aging-0.25) simulation over the whole East Asian region (Table 6). In contrast, POA concentrations were not so sensitive to the aging coefficients. The average POA concentrations were increased by 17 % in the Aging-4 simulation and decreased by 26 % in the Aging-0.25 simulation, both relative to the Aging-on (base) simulation.

5.1.2 Interaction of anthropogenic and biogenic sources

The sensitivity simulations shown in Sects. 5.1.2 and 5.2 are summarized in Fig. 9. The simulation results with aging processes from biogenic sources only (no aging treatment for SIVOCs and anthropogenic OVOCs) are shown in Fig. 8a and Table 6

Title Page

Abstract | Introduction

Conclusions | References

Tables | Figures

|◄ | ►|

◄ | ►

Back | Close

Full Screen / Esc

Printer-friendly Version

Interactive Discussion

(the Aging-bio simulation in Table 4). The contribution of aging processes from anthropogenic sources (ANaging) can be estimated from the difference in OA concentrations between the Aging-on (base case) and Aging-bio simulations (Fig. 9). As expected, the impact of ANaging on OPOA and ASOA over the outer domain was very large: ANaging enhanced OPOA concentrations from 0.0 to 0.37 μg m^{-3} and ASOA concentrations from 0.038 to 0.33 μg m^{-3} (+780 %) (Table 6). ANaging also enhanced POA concentrations moderately (+20 %, Table 6).

BSOA concentrations were also enhanced considerably (+45 %) by ANaging (Table 6). This is because ANaging produced large amounts of low-volatile organic vapors and OA from anthropogenic VOCs and SIVOCs, and these vapors shifted the gas-particle partitioning ratio of BSOA to the particulate phase. Therefore, ANaging is very important for OA formation from both anthropogenic and biogenic sources.

These results show that BSOA concentrations were substantially enhanced by OA models that can represent realistic OA concentrations from anthropogenic OA in the atmosphere (the VBS scheme in case of this study), even if we do not change the treatment of BSOA formation processes in the model. In this study, the importance of this effect was shown for springtime over East Asia, where anthropogenic and biogenic emissions interact closely. Similar interaction is expected over other large emission sources such as the United States and Europe, implying the importance of ANaging to BSOA concentrations on hemispherical and global scales. Therefore, to obtain more accurate simulations of BSOA, which is considered to be dominant globally, it is important to use a realistic OA formation scheme for anthropogenic sources.

Figure 8a also shows the simulation results with aging processes from anthropogenic sources only (the Aging-an simulation in Table 4). We can estimate the contribution of aging processes from biogenic sources (BIOaging) by the difference in OA between the Aging-on (base case) and Aging-an simulations (Fig. 9). BIOaging slightly influenced (less than 4–7 %) POA, OPOA, and ASOA, whereas it is important for BSOA (increased by 210 %). Therefore, the enhancement of anthropogenic OA by aging processes of

biogenic VOCs is limited. The difference in the importance of ANaging and BIOaging is because anthropogenic sources are dominant over East Asia (Fig. 8b).

5.2 Estimation of controllable OA

We estimate the contribution of OA influenced by anthropogenic emission sources (i.e., controllable OA). Here, we assume that biomass burning emissions are not anthropogenic (not controllable) sources, following the treatment in Carlton et al. (2010). For estimating the contribution of controllable OA over East Asia, we conducted sensitivity simulations with various amounts of anthropogenic emissions ranging from 0 % to 200 % of base case emissions for both gaseous (CO, NO_x, SO_2, VOCs, and primary SIVOCs) and aerosol species (POA and black carbon). Other settings were similar to the base case simulation. Biomass burning, biogenic, and volcanic emissions were not changed in these sensitivity simulations.

Period-averaged POA, OPOA, and ASOA concentrations normalized by those in the base case simulation increased almost linearly with anthropogenic emissions over the outer domain in the sensitivity simulations, except for the range of anthropogenic emissions from 0 to 50 %, where the contribution from biomass burning sources dominated (Fig. 10). In the simulation without anthropogenic emissions, POA, OPOA, and ASOA decreased to 20 %, 9 %, and 2 %, respectively, of the base case simulation. This is because the reduction of anthropogenic VOCs, NO_x, and POA lead to OA reduction by changing both VOC concentrations and their oxidation rates, and gas-particle partitioning of organic compounds. Controllable OA concentrations can be estimated from the differences in OA between the simulations with (100 %) and without (0 %) anthropogenic emissions (Fig. 9). The fractions of controllable POA, OPOA, and ASOA were 80 %, 91 %, and 98 %, respectively, in our simulations over all of East Asia.

The fractions of POA, OPOA, and ASOA in the simulation without anthropogenic emissions (20 %, 9 %, and 2 % of the base case) were smaller than the fractions expected from emissions, because biomass burning sources account for 30 % of OA emissions and 10 % of aromatics emissions over the outer domain (Fig. 3c and d).

An important reason for these smaller fractions was the lower OH concentrations (by a factor of 3) and resulting slower rates of oxidation of organic vapors in the simulation without anthropogenic emissions compared with the base case simulation. In fact, the fraction of low-volatile organics (sum of vapors and aerosols) was smaller in the simulation without anthropogenic emissions (not shown).

BSOA mass concentrations were positively related to the amounts of anthropogenic emissions, though the relationship is weaker than POA, OPOA, and ASOA (green line in Fig. 10). The fraction of controllable BSOA was 78 % in our estimation; thus a large portion of BSOA was formed through the influence of anthropogenic sources (the enhancement of anthropogenic VOCs, NO_x, and preexisting OA) over East Asia.

The period-averaged controllable OA concentrations over the outer domain were $1.12\,\mu g\,m^{-3}$ and were higher than the sum of POA, OPOA, and ASOA concentrations ($0.94\,\mu g\,m^{-3}$). The fraction of controllable OA was 87 % (Fig. 11a), suggesting that most of OA was controllable and formed anthropogenically in springtime over all of East Asia. The fraction of controllable OA was more than 90 % over most of India and China and its outflow regions and 60–80 % even over Southeast Asia, where BSOA concentrations were high (Fig. 11c).

Carlton et al. (2010) estimated that more than 50 % of BSOA in the eastern United States was controllable. Global modeling studies showed that only 31 % (Tsigaridis et al., 2006) and 21 % (Hoyle et al., 2009) of the simulated SOA increase from the pre-industrial period to the present was formed directly from anthropogenic VOC, and that the vast majority of the remainder was BSOA enhanced by anthropogenic sources (Hoyle et al., 2011). Spracklen et al. (2011) made top-down estimates of a global SOA budget using both AMS measurements and global model simulations: these estimates suggested that 71 % of SOA formed in the atmosphere was controllable. The contribution of controllable OA estimated in this study is higher than these estimates. The higher contribution of controllable OA in this study is because anthropogenic sources are dominant over East Asia and OA is enhanced considerably by aging processes of organic vapors from anthropogenic sources (Sect. 5.1.2).

Our estimation of the controllable OA fraction may have large uncertainties because biomass burning emissions are still highly uncertain over East Asia (Matsui et al., 2013a). The estimation may also be highly sensitive to the simulation periods because of large seasonal and interannual variations of biomass burning emissions over East Asia (Matsui et al., 2013a).

Without aging processes, the domain- and period averaged controllable OA was $0.18 \, \mu g \, m^{-3}$, and the fraction of controllable OA was 75 % (Fig. 11b). The fraction was lower than that in the base case simulation with aging processes. This is because the fraction of OPOA and ASOA, which are mostly formed from anthropogenic sources, is larger in the base case simulation. Both the amounts (from 0.18 to $1.12 \, \mu g \, m^{-3}$) and the fraction (from 75 % to 87 %) of controllable OA were increased by aging processes of organic vapors over East Asia.

6 Summary and conclusions

We simulated OA concentrations over East Asia and its outflow region by using the VBS approach. Model simulations were evaluated via comparisons with AMS measurements in and around Tokyo (at the Komaba and Kisai sites during the IMPACT-2 campaign in summer 2003 and the IMPACT-L campaign in summer 2004) and over the outflow region in East Asia (at the Fukue and Hedo sites during the A-FORCE campaign in spring 2009).

Model simulations with aging processes of organic vapors (SIVOCs and OVOCs) reasonably well reproduced mass concentrations, temporal variations, and formation efficiency (i.e., SOA/O_3 and OA/SO_4 ratio) of observed OA: the model reproduced SOA concentrations to within 25 % during the IMPACT campaign (NMB of -21 % and -13 % at Komaba and Kisai, respectively), the SOA/O_3 ratio to within 25 % at Komaba and Kisai, OA concentrations to within 15 % at Fukue and to within a factor of 2 at Hedo, and the OA/SO_4 ratio to within 30 % at Fukue and Hedo. In contrast, the simulations without the aging processes did not capture these features. The model without

the aging processes severely underestimated mass concentrations (by 76–88 %) and formation efficiencies of OA (by 80–90 %) at the 4 measurement sites. The oxidation of organic vapors is therefore essential for realistic OA simulations over East Asia.

Concentrations of simulated POA and total SOA (OPOA + ASOA + BSOA) peaked over northern and central China and Southeast Asia, corresponding to large source regions of anthropogenic and biomass burning emissions. Concentrations of ASOA (BSOA) were high over central and northern China (Southeast Asia and southern China). Simulated OA concentrations at an altitude of 1 km over all of East Asia were highly sensitive to aging processes of organic vapors: relative to the results of simulations without aging, total OA concentrations increased from 0.24 to 1.28 $\mu g\,m^{-3}$ (+440 %). Aging processes also changed OA chemical composition: in the simulation with the aging processes, the contributions of OPOA and ASOA were 29 % and 26 %, respectively, of total OA, whereas in the simulation without the aging processes, about 70 % of total OA was POA.

We also examined the importance of the aging processes of organic vapors from anthropogenic (ANaging) and biogenic sources (BIOaging). ANaging was very important for the enhancement of OA formation from both anthropogenic and biogenic sources. ANaging enhanced BSOA concentrations considerably (+45 %), while the enhancement of OPOA and ASOA (SOA from anthropogenic sources) by BIOaging was very limited (less than 4–7 %). The difference in the importance of ANaging and BIOaging is because anthropogenic sources are dominant over East Asia. These results show that BSOA concentrations are substantially enhanced by OA models that can simulate realistic OA concentrations from anthropogenic sources in the atmosphere, even if we do not change the treatment of BSOA formation processes in the model. Therefore, to obtain more accurate simulations of BSOA, which is considered to be dominant globally, it is important to use a realistic OA formation scheme for anthropogenic sources.

The fraction of controllable OA estimated in our simulations was 87 %, suggesting that most OA was controllable and formed anthropogenically in springtime over all of East Asia. The fractions of controllable POA, OPOA, ASOA, and BSOA were 80 %,

VBS OA Simulation in East Asia

H. Matsui et al.

91 %, 98 %, and 78 %, respectively, showing that even a large portion of BSOA was formed through the influence of anthropogenic sources (the enhancement of anthropogenic VOCs, NO_x, and preexisting OA). These fractions are higher than the fraction of anthropogenic emissions (70 % of OA emissions and 90 % of aromatics emissions over East Asia during the simulation periods). An important reason for these higher controllable fractions is higher OH concentration resulting in faster oxidation rates of organic vapors by considering anthropogenic sources. Both the amounts (from 0.18 to 1.12 $\mu g\,m^{-3}$) and the fraction (from 75 % to 87 %) of controllable OA were increased by including aging processes of organic vapors over East Asia.

This study is a first step to examine OA concentrations and their spatial distributions and the anthropogenic-biogenic interaction in OA formation over all of East and Southeast Asia and its outflow regions. Further validations of OA, precursor VOCs, and oxidant species especially over southern China and Southeast Asia, where the contribution of biogenic sources are high, are necessary to understand the behavior of OA and the anthropogenic-biogenic interaction over the Asian region more quantitatively.

Discussion Paper | Discussion Paper | Discussion Paper | Discussion Paper |

VBS OA Simulation in East Asia

H. Matsui et al.

Title Page

Abstract | Introduction

Conclusions | References

Tables | Figures

◄ | ►

◄ | ►

Back | Close

Full Screen / Esc

Printer-friendly Version

Interactive Discussion

Discussion Paper | Discussion Paper | Discussion Paper | Discussion Paper

ACPD

14, 6203–6260, 2014

VBS OA Simulation in East Asia

H. Matsui et al.

Title Page

Abstract | Introduction

Conclusions | References

Tables | Figures

◄◄ | ►►

◄ | ►

Back | Close

Full Screen / Esc

Printer-friendly Version

Interactive Discussion

References

Adhikary, B., Carmichael, G. R., Kulkarni, S., Wei, C., Tang, Y., D'Allura, A., Mena-Carrasco, M., Streets, D. G., Zhang, Q., Pierce, R. B., Al-Saadi, J. A., Emmons, L. K., Pfister, G. G., Avery, M. A., Barrick, J. D., Blake, D. R., Brune, W. H., Cohen, R. C., Dibb, J. E., Fried, A., Heikes, B. G., Huey, L. G., O'Sullivan, D. W., Sachse, G. W., Shetter, R. E., Singh, H. B., Campos, T. L., Cantrell, C. A., Flocke, F. M., Dunlea, E. J., Jimenez, J. L., Weinheimer, A. J., Crounse, J. D., Wennberg, P. O., Schauer, J. J., Stone, E. A., Jaffe, D. A., and Reid-miller, D. R.: A regional scale modeling analysis of aerosol and trace gas distributions over the eastern Pacific during the INTEX-B field campaign, Atmos. Chem. Phys., 10, 2091–2115, doi:10.5194/acp-10-2091-2010, 2010.

Ahmadov, R., McKeen, S. A., Robinson, A. L., Bahreini, R., Middlebrook, A. M., de Gouw, J. A., Meagher, J., Hsie, E.-Y., Edgerton, E., Shaw, S., and Trainer, M.: A volatility basis set model for summertime secondary organic aerosols over the eastern United States in 2006, J. Geophys. Res., 117, D06301, doi:10.1029/2011JD016831, 2012.

Athanasopoulou, E., Vogel, H., Vogel, B., Tsimpidi, A. P., Pandis, S. N., Knote, C., and Fountoukis, C.: Modeling the meteorological and chemical effects of secondary organic aerosols during an EUCAARI campaign, Atmos. Chem. Phys., 13, 625–645, doi:10.5194/acp-13-625-2013, 2013.

Andersson-Sköld, Y. and Simpson, D.: Secondary organic aerosol formation in northern Europe: a model study, J. Geophys. Res., 106, 7357–7374, doi:10.1029/2000JD900656, 2001.

Bahadur, R., Habib, G., and Russell, L. M.: Climatology of $PM_{2.5}$ organic carbon concentrations from a review of ground-based atmospheric measurements by evolved gas analysis, Atmos. Environ., 43, 1591–1602, 2009.

Bergström, R., Denier van der Gon, H. A. C., Prévôt, A. S. H., Yttri, K. E., and Simpson, D.: Modelling of organic aerosols over Europe (2002–2007) using a volatility basis set (VBS) framework: application of different assumptions regarding the formation of secondary organic aerosol, Atmos. Chem. Phys., 12, 8499–8527, doi:10.5194/acp-12-8499-2012, 2012.

Binkowski, F. S and Shankar, U.: The regional particulate matte model: 1. Model description and preliminary results, J. Geophys. Res., 100, 26191–26209, 1995.

Bond, T. C., Doherty, S. J., Fahey, D. W., Forster, P. M., Berntsen, T., DeAngelo, B. J., Flanner, M. G., Ghan, S., Kärcher, B., Koch, D., Kinne, S., Kondo, Y., Quinn, P. K., Sarofim, M. C., Schultz, M. G., Schulz, M., Venkataraman, C., Zhang, H., Zhang, S., Bellouin, N., Gut-

tikunda, S. K., Hopke, P. K., Jacobson, M. Z., Kaiser, J. W., Klimont, Z., Lohmann, U., Schwarz, J. P., Shindell, D., Storelvmo, T., Warren, S. G., and Zender, C. S.: Bounding the role of black carbon in the climate system: a scientific assessment, J. Geophys. Res. Atmos., 118, 5380–5552, doi:10.1002/jgrd.50171, 2013.

5 Carlton, A. G., Pinder, R. W., Bhave, P. V., and Pouliot, G. A.: To what extent can biogenic SOA be controlled?, Environ. Sci. Technol., 44, 3376–3380, 2010.

Carmichael, G. R., Tang, Y., Kurata, G., Uno, I., Streets, D., Woo, J.-H., Huang, H., Yienger, J., Lefer, B., Shetter, R., Blake, D., Atlas, E., Fried, A., Apel, E., Eisele, F., Cantrell, C., Avery, M., Barrick, J., Sachse, G., Brune, W., Sandholm, S., Kondo, Y., Singh, H., Talbot, R., Bandy., A.,

10 Thorton, D., Clarke, A., and Heikes, B.: Regional-scale chemical transport modeling in support of the analysis of observations obtained during the TRACE-P experiment, J. Geophys. Res., 108, 8823, doi:10.1029/2002JD003117, 2003.

Carter, W. P. L.: Documentation of the SAPRC-99 Chemical Mechanism for VOC Reactivity Assessment, Report to the California Air Resources Board. College of Engineering, Center

15 for Environmental Research and Technology, University of California at Riverside, C A. Contracts 92–329 and 95–308, available at: http://www.cert.ucr.edu/~carter/reactdat.htm (last access: 27 February 2014), 2000.

Chung, S. and Seinfeld, J. H.: Global distribution and climate forcing of carbonaceous aerosols, J. Geophys. Res., 107, 4407, doi:10.1029/2001JD001397, 2002.

20 de Gouw, J. and Jimenez, J. L.: Organic aerosols in the Earth's atmosphere, Environ. Sci. Technol., 43, 7614–7618, 2009.

Dentener, F., Kinne, S., Bond, T., Boucher, O., Cofala, J., Generoso, S., Ginoux, P., Gong, S., Hoelzemann, J. J., Ito, A., Marelli, L., Penner, J. E., Putaud, J.-P., Textor, C., Schulz, M., van der Werf, G. R., and Wilson, J.: Emissions of primary aerosol and precursor gases in

25 the years 2000 and 1750 prescribed data-sets for AeroCom, Atmos. Chem. Phys., 6, 4321–4344, doi:10.5194/acp-6-4321-2006, 2006.

Donahue, N. M., Robinson, A. L., Stanier, C. O., and Pandis, S. N.: Coupled partitioning, dilution, and chemical aging of semivolatile organics, Environ. Sci. Technol., 40, 2635–2643, 2006.

30 Donahue, N. M., Epstein, S. A., Pandis, S. N., and Robinson, A. L.: A two-dimensional volatility basis set: 1. organic-aerosol mixing thermodynamics, Atmos. Chem. Phys., 11, 3303–3318, doi:10.5194/acp-11-3303-2011, 2011.

Dunlea, E. J., DeCarlo, P. F., Aiken, A. C., Kimmel, J. R., Peltier, R. E., Weber, R. J., Tomlinson, J., Collins, D. R., Shinozuka, Y., McNaughton, C. S., Howell, S. G., Clarke, A. D., Emmons, L. K., Apel, E. C., Pfister, G. G., van Donkelaar, A., Martin, R. V., Millet, D. B., Heald, C. L., and Jimenez, J. L.: Evolution of Asian aerosols during transpacific transport in INTEX-B, Atmos. Chem. Phys., 9, 7257–7287, doi:10.5194/acp-9-7257-2009, 2009.

Easter, R. C., Ghan, S. J., Zhang, Y., Saylor, R. D., Chapman, E. G., Laulainen, N. S., Abdul-Razzak, H., Leung, L. R., Bian, X., and Zaveri, R. A.: MIRAGE: model description and evaluation of aerosols and trace gases, J. Geophys. Res., 109, D20210, doi:10.1029/2004JD004571, 2004.

Ervens, B., Carlton, A. G., Turpin, B. J., Altieri, K. E., Kreidenweis, S. M., and Feingold, G.: Secondary organic aerosol yields from cloud-processing of isoprene oxidation products, Geophys. Res. Lett., 35, L02816, doi:10.1029/2007GL031828, 2008.

Ervens, B. and Volkamer, R.: Glyoxal processing by aerosol multiphase chemistry: towards a kinetic modeling framework of secondary organic aerosol formation in aqueous particles, Atmos. Chem. Phys., 10, 8219–8244, doi:10.5194/acp-10-8219-2010, 2010.

Ervens, B., Turpin, B. J., and Weber, R. J.: Secondary organic aerosol formation in cloud droplets and aqueous particles (aqSOA): a review of laboratory, field and model studies, Atmos. Chem. Phys., 11, 11069–11102, doi:10.5194/acp-11-11069-2011, 2011.

Fahey, K. M. and Pandis, S. N.: Optimizing model performance: variable size resolution in cloud chemistry modeling, Atmos. Environ., 35, 4471–4478, 2001.

Farina, S. C., Adams, P. J., and Pandis, S. N.: Modeling global secondary organic aerosol formation and processing with the volatility basis set: implications for anthropogenic secondary organic aerosol, J. Geophys. Res., 115, D09202, doi:10.1029/2009JD013046, 2010.

Fast, J. D., Gustafson Jr., W. I., Easter, R. C., Zaveri, R. A., Barnard, J. C., Chapman, E. G., Grell, G. A., and Peckham, S. E.: Evolution of ozone, particulates, and aerosol direct radiative forcing in the vicinity of Houston using a fully coupled meteorology–chemistry–aerosol model, J. Geophys. Res., 111, D21305, doi:10.1029/2005JD006721, 2006.

Fountoukis, C., Racherla, P. N., Denier van der Gon, H. A. C., Polymeneas, P., Charalampidis, P. E., Pilinis, C., Wiedensohler, A., Dall'Osto, M., O'Dowd, C., and Pandis, S. N.: Evaluation of a three-dimensional chemical transport model (PMCAMx) in the European domain during the EUCAARI May 2008 campaign, Atmos. Chem. Phys., 11, 10331–10347, doi:10.5194/acp-11-10331-2011, 2011.

Title Page

Abstract | Introduction

Conclusions | References

Tables | Figures

◄◄ | ►►

◄ | ►

Back | Close

Full Screen / Esc

Printer-friendly Version

Interactive Discussion

George, I. J., Vlasenko, A., Slowik, J. G., Broekhuizen, K., and Abbatt, J. P. D.: Hetero-geneous oxidation of saturated organic aerosols by hydroxyl radicals: uptake kinetics, condensed-phase products, and particle size change, Atmos. Chem. Phys., 7, 4187–4201, doi:10.5194/acp-7-4187-2007, 2007.

George, I. J., Slowik, J., and Abbatt, J. P. D.: Chemical aging of ambient organic aerosol from heterogeneous reaction with hydroxyl radicals, Geophys. Res. Lett., 35, L13811, doi:10.1029/2008GL033884, 2008.

Goldstein, A. H. and Galbally, I. E.: Known and unexplored organic constituents in the Earth's atmosphere, Environ. Sci. Technol., 41, 1514–1521, 2007.

Grell, G. A., Peckham, S. E., Schmitz, R., McKeen, S. A., Frost, G., Skamarock, W. C., and Eder, B.: Fully coupled "online" chemistry within the WRF model, Atmos. Environ., 39, 6957–6975, 2005.

Guenther, A., Karl, T., Harley, P., Wiedinmyer, C., Palmer, P. I., and Geron, C.: Estimates of global terrestrial isoprene emissions using MEGAN (Model of Emissions of Gases and Aerosols from Nature), Atmos. Chem. Phys., 6, 3181–3210, doi:10.5194/acp-6-3181-2006, 2006.

Hallquist, M., Wenger, J. C., Baltensperger, U., Rudich, Y., Simpson, D., Claeys, M., Dom-men, J., Donahue, N. M., George, C., Goldstein, A. H., Hamilton, J. F., Herrmann, H., Hoff-mann, T., Iinuma, Y., Jang, M., Jenkin, M. E., Jimenez, J. L., Kiendler-Scharr, A., Maen-haut, W., McFiggans, G., Mentel, Th. F., Monod, A., Prévôt, A. S. H., Seinfeld, J. H., Sur-ratt, J. D., Szmigielski, R., and Wildt, J.: The formation, properties and impact of sec-ondary organic aerosol: current and emerging issues, Atmos. Chem. Phys., 9, 5155–5236, doi:10.5194/acp-9-5155-2009, 2009.

Han, Z., Zhang, R., Wang, Q., Wang, W., Cao, J., and Xu, J.: Regional model-ing of organic aerosols over China in summertime, J. Geophys. Res., 113, D11202, doi:10.1029/2007JD009436, 2008.

Heald, C. L., Jacob, D. J., Park, R. J., Russell, L. M., Huebert, B. J., Seinfeld, J. H., Liao, H., and Weber, R. J.: A large organic aerosol source in the free troposphere missing from current models, Geophys. Res. Lett., 32, L18809, doi:10.1029/2005GL023831, 2005.

Heald, C. L., Henze, D. K., Horowitz, L. W., Feddema, J., Lamarque, J.-F., Guenther, A., Hess, P. G., Vitt, F., Seinfeld, J. H., Goldstein, A. H., and Fung, I.: Predicted change in global secondary organic aerosol concentrations in response to future climate, emissions, and land use change, J. Geophys. Res., 113, D05211, doi:10.1029/2007JD009092, 2008.

Title Page

Abstract | Introduction

Conclusions | References

Tables | Figures

|◄ | ►|

◄ | ►

Back | Close

Full Screen / Esc

Printer-friendly Version

Interactive Discussion

Heald, C. L., Ridley, D. A., Kreidenweis, S. M., and Drury, E. E.: Satellite observations cap the atmospheric organic aerosol budget, Geophys. Res. Lett., 37, L24808, doi:10.1029/2010GL045095, 2010.

Heald, C. L., Coe, H., Jimenez, J. L., Weber, R. J., Bahreini, R., Middlebrook, A. M., Russell, L. M., Jolleys, M., Fu, T.-M., Allan, J. D., Bower, K. N., Capes, G., Crosier, J., Morgan, W. T., Robinson, N. H., Williams, P. I., Cubison, M. J., DeCarlo, P. F., and Dunlea, E. J.: Exploring the vertical profile of atmospheric organic aerosol: comparing 17 aircraft field campaigns with a global model, Atmos. Chem. Phys., 11, 12673–12696, doi:10.5194/acp-11-12673-2011, 2011.

Henze, D. K., Seinfeld, J. H., Ng, N. L., Kroll, J. H., Fu, T.-M., Jacob, D. J., and Heald, C. L.: Global modeling of secondary organic aerosol formation from aromatic hydrocarbons: high- vs. low-yield pathways, Atmos. Chem. Phys., 8, 2405–2420, doi:10.5194/acp-8-2405-2008, 2008.

Herndon, S. C., Onasch, T. B., Wood, E. C., Kroll, J. H., Canagaratna, M. R., Jayne, J. T., Zavala, M. A., Knighton, W. B., Mazzoleni, C., Dubey, M. K., Ulbrich, I. M., Jimenez, J. L., Seila, R., de Gouw, J. A., de Foy, B., Fast, J., Molina, L. T., Kolb, C. E., and Worsnop, D. R.: Correlation of secondary organic aerosol with odd oxygen in Mexico City, Geophys. Res. Lett., 35, L15804, doi:10.1029/2008GL034058, 2008.

Hodzic, A., Jimenez, J. L., Madronich, S., Canagaratna, M. R., DeCarlo, P. F., Kleinman, L., and Fast, J.: Modeling organic aerosols in a megacity: potential contribution of semi-volatile and intermediate volatility primary organic compounds to secondary organic aerosol formation, Atmos. Chem. Phys., 10, 5491–5514, doi:10.5194/acp-10-5491-2010, 2010.

Hoyle, C. R., Myhre, G., Berntsen, T. K., and Isaksen, I. S. A.: Anthropogenic influence on SOA and the resulting radiative forcing, Atmos. Chem. Phys., 9, 2715–2728, doi:10.5194/acp-9-2715-2009, 2009.

Hoyle, C. R., Boy, M., Donahue, N. M., Fry, J. L., Glasius, M., Guenther, A., Hallar, A. G., Huff Hartz, K., Petters, M. D., Petäjä, T., Rosenoern, T., and Sullivan, A. P.: A review of the anthropogenic influence on biogenic secondary organic aerosol, Atmos. Chem. Phys., 11, 321–343, doi:10.5194/acp-11-321-2011, 2011.

Huang, H., Ho, K. F., Lee, S. C., Tsang, P. K., Ho, S. S. H., Zou, C. W., Zou, S. C., Cao, J. J., and Xu, H. M.: Characteristics of carbonaceous aerosol in $PM_{2.5}$: Pearl Delta River Region, China, Atmos. Res., 104–105, 227–236, 2012.

VBS OA Simulation in East Asia

H. Matsui et al.

Title Page

Abstract | Introduction

Conclusions | References

Tables | Figures

◄◄ | ►►

◄ | ►

Back | Close

Full Screen / Esc

Printer-friendly Version

Interactive Discussion

Iinuma, Y., Böge, O., Gnauk, T., and Herrmann, H.: Aerosol-chamber study of the α-pinene/O_3 reaction: influence of particle acidity on aerosol yields and products, Atmos. Environ., 38, 761–773, 2004.

Jathar, S. H., Farina, S. C., Robinson, A. L., and Adams, P. J.: The influence of semi-volatile and reactive primary emissions on the abundance and properties of global organic aerosol, Atmos. Chem. Phys., 11, 7727–7746, doi:10.5194/acp-11-7727-2011, 2011.

Jimenez, J. L., Canagaratna, M. R., Donahue, N. M., Prevot, A. S. H., Zhang, Q., Kroll, J. H., DeCarlo, P. F., Allan, J. D., Coe, H., Ng, N. L., Aiken, A. C., Docherty, K. S., Ulbrich, I. M., Grieshop, A. P., Robinson, A. L., Duplissy, J., Smith, J. D., Wilson, K. R., Lanz, V. A., Hueglin, C., Sun, Y. L., Tian, J., Laaksonen, A., Raatikainen, T., Rautiainen, J., Vaattovaara, P., Ehn, M., Kulmala, M., Tomlinson, J. M., Collins, D. R., Cubison, M. J., Dunlea, E. J., Huffman, J. A., Onasch, T. B., Alfarra, M. R., Williams, P. I., Bower, K., Kondo, Y., Schneider, J., Drewnick, F., Borrmann, S., Weimer, S., Demerjian, K., Salcedo, D., Cottrell, L., Griffin, R., Takami, A., Miyoshi, T., Hatakeyama, S., Shimono, A., Sun, J. Y., Zhang, Y. M., Dzepina, K., Kimmel, J. R., Sueper, D., Jayne, J. T., Herndon, S. C., Trimborn, A. M., Williams, L. R., Wood, E. C., Middlebrook, A. M., Kolb, C. E., Baltensperger, U., and Worsnop, D. R.: Evolution of organic aerosols in the atmosphere, Science, 326, 1525–1529, 2009.

Jacobson, M. Z., Turco, R. P., Jensen, E. J., and Toon, O. B.: Modeling coagulation among particles of different composition and size, Atmos. Environ., 28, 1327–1338, 1994.

Jiang, F., Liu, Q., Huang, X. X., Wang, T. J., Zhuang, B. L., and Xie, M.: Regional modeling of secondary organic aerosol over China using WRF/Chem, J. Aerosol Sci., 43, 57–73, 2012.

Kalberer, M., Paulsen, D., Sax, M., Steinbacher, M., Dommen, J., Prevot, A. S. H., Fisseha, R., Weingartner, E., Frankevich, V., Zanobi, R., and Baltensperger, U.: Identification of polymers as major components of atmospheric organic aerosols, Science, 303, 1659–1662, 2004.

Kanakidou, M., Seinfeld, J. H., Pandis, S. N., Barnes, I., Dentener, F. J., Facchini, M. C., Van Dingenen, R., Ervens, B., Nenes, A., Nielsen, C. J., Swietlicki, E., Putaud, J. P., Balkanski, Y., Fuzzi, S., Horth, J., Moortgat, G. K., Winterhalter, R., Myhre, C. E. L., Tsigaridis, K., Vignati, E., Stephanou, E. G., and Wilson, J.: Organic aerosol and global climate modelling: a review, Atmos. Chem. Phys., 5, 1053–1123, doi:10.5194/acp-5-1053-2005, 2005.

Kanaya, Y., Cao, R., Akimoto, H., Fukuda, M., Komazaki, Y., Yokouchi, Y., Koike, M., Tanimoto, H., Takegawa, N., and Kondo, Y.: Urban photochemistry in central Tokyo: 1. Observed and modeled OH and HO_2 radical concentrations during the winter and summer of 2004, J. Geophys. Res., 112, D21312, doi:10.1029/2007JD008670, 2007.

Title Page

Abstract | Introduction

Conclusions | References

Tables | Figures

|◄ | ►|

◄ | ►

Back | Close

Full Screen / Esc

Printer-friendly Version

Interactive Discussion

VBS OA Simulation in East Asia

H. Matsui et al.

Title Page

Abstract | Introduction

Conclusions | References

Tables | Figures

◄ | ►

◄ | ►

Back | Close

Full Screen / Esc

Printer-friendly Version

Interactive Discussion

Kannari, A., Baba, T., Ueda, H., Tonooka, Y., and Matsuda, K.: Development of a grid database on atmospheric pollutants emissions in Japan, J. Jpn. Soc. Atmos. Environ., 39, 257–271, 2004 (in Japanese).

Kondo, Y., Komazaki, Y., Miyazaki, Y., Moteki, N., Takegawa, N., Kodama, D., Deguchi, S., Nogami, M., Fukuda, M., Miyakawa, T., Morino, Y., Koike, M., Sakurai, H., and Ehara, K.: Temporal variations of elemental carbon in Tokyo, J. Geophys. Res., 111, D12205, doi:10.1029/2005JD006257, 2006.

Kondo, Y., Miyazaki, Y., Takegawa, N., Miyakawa, T., Weber, R. J., Jimenez, J. L., Zhang, Q., and Worsnop, D. R.: Oxygenated and water-soluble organic aerosols in Tokyo, J. Geophys. Res., 112, D01203, doi:10.1029/2006JD007056, 2007.

Kondo, Y., Morino, Y., Fukuda, M., Kanaya, Y., Miyazaki, Y., Takegawa, N., Tanimoto, H., McKenzie, R., Johnston, P., Blake, D. R., Murayama, T., and Koike, M.: Formation and transport of oxidized reactive nitrogen, ozone, and secondary organic aerosol in Tokyo, J. Geophys. Res., 113, D21310, doi:10.1029/2008JD010134, 2008.

Kondo, Y., Takegawa, N., Matsui, H., Miyakawa, T., Koike, M., Miyazaki, Y., Kanaya, Y., Mochida, M., Kuwata, M., Morino, Y., and Shiraiwa, M.: Formation and transport of aerosols in Tokyo in relation to their physical and chemical properties: a review, J. Meteorol. Soc. Jpn., 88, 597–624, 2010.

Kondo, Y., Oshima, N., Kajino, M., Mikami, R., Moteki, N., Takegawa, N., Verma, R. L., Kajii, Y., Kato, S., and Takami, A.: Emissions of black carbon in East Asia estimated from observations at a remote site in the East China Sea, J. Geophys. Res., 116, D16201, doi:10.1029/2011JD015637, 2011.

Koo, B., Ansari, A. S., and Pandis, S. N.: Integrated approaches to modeling the organic and inorganic atmospheric aerosol components, Atmos. Environ., 37, 4757–4768, 2003.

Kroll, J. H., Smith, J. D., Che, D. L., Kessler, S. H., Worsnop, D. R., and Wilson, K. R.: Measurement of fragmentation and functionalization pathways in the heterogeneous oxidation of oxidized organic aerosol, Phys. Chem. Chem. Phys., 11, 8005–8014, 2009.

Lane, T. E., Donahue, N. M., and Pandis, S. N.: Effect of NO_x on secondary organic aerosol concentrations, Environ. Sci. Technol., 42, 6022–6027, 2008a.

Lane, T. E., Donahue, N. M., and Pandis, S. N.: Simulating secondary organic aerosol formation using the volatility basis-set approach in a chemical transport model, Atmos. Environ., 42, 7439–7451, 2008b.

Levine, S. Z. and Schwartz, S. E.: In-cloud and below-cloud scavenging of nitric acid vapor, Atmos. Environ., 16, 1725–1734, 1982.

Liao, H. and Seinfeld, J. H.: Global impacts of gas-phase chemistry-aerosol interactions on direct radiative forcing by anthropogenic aerosols and ozone, J. Geophys. Res., 110, D18208, doi:10.1029/2005JD005907, 2005.

Li, G., Zavala, M., Lei, W., Tsimpidi, A. P., Karydis, V. A., Pandis, S. N., Canagaratna, M. R., and Molina, L. T.: Simulations of organic aerosol concentrations in Mexico City using the WRF-CHEM model during the MCMA-2006/MILAGRO campaign, Atmos. Chem. Phys., 11, 3789–3809, doi:10.5194/acp-11-3789-2011, 2011.

Li, N., Fu, T.-M., Cao, J., Lee, S., Huang, X.-F., He, L.-Y., Ho, K.-F., Fu, J. S., and Lam, Y.-F.: Sources of secondary organic aerosols in the Pearl River Delta region in fall: contributions from the aqueous reactive uptake of dicarbonyls, Atmos. Environ., 76, 200–207, 2013.

Lim, Y. B., Tan, Y., Perri, M. J., Seitzinger, S. P., and Turpin, B. J.: Aqueous chemistry and its role in secondary organic aerosol (SOA) formation, Atmos. Chem. Phys., 10, 10521–10539, doi:10.5194/acp-10-10521-2010, 2010.

Lin, G., Penner, J. E., Sillman, S., Taraborrelli, D., and Lelieveld, J.: Global modeling of SOA formation from dicarbonyls, epoxides, organic nitrates and peroxides, Atmos. Chem. Phys., 12, 4743–4774, doi:10.5194/acp-12-4743-2012, 2012.

Liu, J., Mauzerall, D. L., and Horowitz, L. W.: Source-receptor relationships between East Asian sulfur dioxide emissions and Northern Hemisphere sulfate concentrations, Atmos. Chem. Phys., 8, 3721–3733, doi:10.5194/acp-8-3721-2008, 2008.

Liu, J., Horowitz, L. W., Fan, S., Carlton, A. G., and Levy II, H.: Global in-cloud production of secondary organic aerosols: implementation of a detailed chemical mechanism in the GFDL atmospheric model AM3, J. Geophys. Res., 117, D15303, doi:10.1029/2012JD017838, 2012.

Matsui, H., Koike, M., Takegawa, N., Kondo, Y., Griffin, R. J., Miyazaki, Y., Yokouchi, Y., and Ohara, T.: Secondary organic aerosol formation in urban air: temporal variations and possible contributions from unidentified hydrocarbons, J. Geophys. Res., 114, D04201, doi:10.1029/2008JD010164, 2009a.

Matsui, H., Koike, M., Kondo, Y., Takegawa, N., Kita, K., Miyazaki, Y., Hu, M., Chang, S.-Y., Blake, D. R., Fast, J. D., Zaveri, R. A., Streets, D. G., Zhang, Q., and Zhu, T.: Spatial and temporal variations of aerosols around Beijing in summer 2006: model evaluation and source apportionment, J. Geophys. Res., 114, D00G13, doi:10.1029/2008JD010906, 2009b.

Title Page

Abstract | Introduction

Conclusions | References

Tables | Figures

|◀ | ▶|

◀ | ▶

Back | Close

Full Screen / Esc

Printer-friendly Version

Interactive Discussion

Matsui, H., Koike, M., Kondo, Y., Takegawa, N., Fast, J. D., Pöschl, U., Garland, R. M., Andreae, M. O., Wiedensohler, A., Sugimoto, N., and Zhu, T.: Spatial and temporal variations of aerosols around Beijing in summer 2006: 2. Local and column aerosol optical properties, J. Geophys. Res., 115, D22207, doi:10.1029/2010JD013895, 2010.

Matsui, H., Kondo, Y., Moteki, N., Takegawa, N., Sahu, L. K., Zhao, Y., Fuelberg, H. E., Sessions, W. R., Diskin, G., Blake, D. R., Wisthaler, A., and Koike, M.: Seasonal variation of the transport of black carbon aerosol from the Asian continent to the Arctic during the ARCTAS aircraft campaign, J. Geophys. Res., 116, D05202, doi:10.1029/2010JD015067, 2011a.

Matsui, H., Kondo, Y., Moteki, N., Takegawa, N., Sahu, L. K., Koike, M., Zhao, Y., Fuelberg, H. E., Sessions, W. R., Diskin, G., Anderson, B. E., Blake, D. R., Wisthaler, A., Cubison, M. J., and Jimenez, J. L.: Accumulation-mode aerosol number concentrations in the Arctic during the ARCTAS aircraft campaign: long-range transport of polluted and clean air from the Asian continent, J. Geophys. Res., 116, D20217, doi:10.1029/2011JD016189, 2011b.

Matsui, H., Koike, M., Kondo, Y., Takegawa, N., Wiedensohler, A., Fast, J. D., and Zaveri, R. A.: Impact of new particle formation on the concentrations of aerosols and cloud condensation nuclei around Beijing, J. Geophys. Res., 116, D19208, doi:10.1029/2011JD016025, 2011c.

Matsui, H., Koike, M., Kondo, Y., Oshima, N., Moteki, N., Kanaya, Y., Takami, A., and Irwin, M.: Seasonal variations of Asian black carbon outflow to the Pacific: contribution from anthropogenic sources in China and biomass burning sources in Siberia and Southeast Asia, J. Geophys. Res. Atmos., 118, 9948–9967, doi:10.1002/jgrd.50702, 2013a.

Matsui, H., Koike, M., Kondo, Y., Moteki, N., Fast, J. D., and Zaveri, R. A.: Development and validation of a black carbon mixing state resolved three-dimensional model: aging processes and radiative impact, J. Geophys. Res. Atmos., 118, 2304–2326, 2013b.

Matsui, H., Koike, M., Takegawa, N., Kondo, Y., Takami, A., Takamura, T., Yoon, S., Kim, S.-W., Lim, H.-C., and Fast, J. D.: Spatial and temporal variations of new particle formation in East Asia using an NPF-explicit WRF-chem model: north-south contrast in new particle formation frequency, J. Geophys. Res. Atmos., 118, 11647–11663, doi:10.1002/jgrd.50821, 2013c.

McKeen, S., Chung, S. H., Wilczak, J., Grell, G., Djalalova, I., Peckham, S., Gong, W., Bouchet, V., Moffet, R., Tang, Y., Carmichael, G. R., Mathur, R., and Yu, S.: Evaluation of several PM$_{2.5}$ forecast models using data collected during the ICARTT/NEAQS 2004 field study, J. Geophys. Res., 112, D10S20, doi:10.1029/2006JD007608, 2007.

Title Page

Abstract | Introduction

Conclusions | References

Tables | Figures

◀◀ | ▶▶

◀ | ▶

Back | Close

Full Screen / Esc

Printer-friendly Version

Interactive Discussion

Murphy, B. N., Donahue, N. M., Fountoukis, C., and Pandis, S. N.: Simulating the oxygen content of ambient organic aerosol with the 2D volatility basis set, Atmos. Chem. Phys., 11, 7859–7873, doi:10.5194/acp-11-7859-2011, 2011.

Murphy, B. N., Donahue, N. M., Fountoukis, C., Dall'Osto, M., O'Dowd, C., Kiendler-Scharr, A., and Pandis, S. N.: Functionalization and fragmentation during ambient organic aerosol aging: application of the 2-D volatility basis set to field studies, Atmos. Chem. Phys., 12, 10797–10816, doi:10.5194/acp-12-10797-2012, 2012.

Nakajima, T., Yoon, S.-C., Ramanathan, V., Shi, G.-Y., Takemura, T., Higurashi, A., Takamura, T., Aoki, K., Sohn, B.-J., Kim, S.-W., Tsuruta, H., Sugimoto, N., Shimizu, A., Tanimoto, H., Sawa, Y., Lin, N.-H., Lee, C.-T., Goto, D., and Schutgens, N.: Overview of the Atmospheric Brown Cloud East Asian Regional Experiment 2005 and a study of the aerosol direct radiative forcing in east Asia, J. Geophys. Res., 112, D24S91, doi:10.1029/2007JD009009, 2007.

O'Donnell, D., Tsigaridis, K., and Feichter, J.: Estimating the direct and indirect effects of secondary organic aerosols using ECHAM5-HAM, Atmos. Chem. Phys., 11, 8635–8659, doi:10.5194/acp-11-8635-2011, 2011.

Odum, J. R., Hoffmann, T., Bowman, F., Collins, D., Flagan, R. C., and Seinfeld, J. H.: Gas/particle partitioning and secondary organic aerosol yields, Environ. Sci. Technol., 30, 2580–2585, 1996.

Odum, J. R., Jungkamp, T. P. W., Griffin, R. J., Flagan, R. C., and Seinfeld, J. H.: The atmospheric aerosol-forming potential of whole gasoline vapor, Science, 276, 96–99, 1997.

Oshima, N., Kondo, Y., Moteki, N., Takegawa, N., Koike, M., Kita. K., Matsui, H., Kajino, M., Nakamura, H., Jung, J. S., and Kim, Y. J.: Wet removal of black carbon in Asian outflow: aerosol Radiative Forcing in East Asia (A-FORCE) aircraft campaign, J. Geophys. Res., 117, D03204, doi:10.1029/2011JD016552, 2012.

Oshima., N., Koike, M., Kondo, Y., Nakamura, H., Moteki, N., Matsui, H., Takegawa, N., and Kita, K.: Vertical transport mechanisms of black carbon over East Asia in spring during the A-FORCE aircraft campaign, J. Geophys. Res. Atmos., 118, 13175–13198, doi:10.1002/2013JD020262, 2013.

Pye, H. O. T., Chan, A. W. H., Barkley, M. P., and Seinfeld, J. H.: Global modeling of organic aerosol: the importance of reactive nitrogen (NO_x and NO_3), Atmos. Chem. Phys., 10, 11261–11276, doi:10.5194/acp-10-11261-2010, 2010.

VBS OA Simulation in East Asia

H. Matsui et al.

Title Page

Abstract	Introduction
Conclusions	References
Tables	Figures

◀◀ ▶▶

◀ ▶

Back Close

Full Screen / Esc

Printer-friendly Version

Interactive Discussion

Pye, H. O. T. and Seinfeld, J. H.: A global perspective on aerosol from low-volatility organic compounds, Atmos. Chem. Phys., 10, 4377–4401, doi:10.5194/acp-10-4377-2010, 2010.

Ramanathan, V., Crutzen, P. J., Kiehl, J. T., and Rosenfeld, D.: Aerosols, climate, and the hydrological cycle, Science, 294, 2119–2124, 2001.

Robinson, A. L., Donahue, N. M., Shrivastava, M. K., Weitkamp, E. A., Sage, A. M., Grieshop, A. P., Lane, T. E., Pierce, J. R., and Pandis, S. N.: Rethinking organic aerosols: semivolatile emissions and photochemical aging, Science, 315, 1259–1262, 2007.

Sahu, L. K., Kondo, Y., Miyazaki, Y., Pongkiatkul, P., and Kim Oanh, N. T.: Seasonal and diurnal variations of black carbon and organic carbon aerosols in Bangkok, J. Geophys. Res., 116, D15302, doi:10.1029/2010JD015563, 2011.

Schell, B., Ackermann, I. J., Hass, H., Binkowski, F. S., and Ebel, A.: Modeling the formation of secondary organic aerosol within a comprehensive air quality model system, J. Geophys. Res., 106, 28275–28293, doi:10.1029/2001JD000384, 2001.

Shirai, T., Yokouchi, Y., Blake, D. R., Kita, K., Izumi, K., Koike, M., Komazaki, Y., Miyazaki, Y., Fukuda, M., and Kondo, Y.: Seasonal variations of atmospheric C_2–C_7 nonmethane hydrocarbons in Tokyo, J. Geophys. Res., 112, D24305, doi:10.1029/2006JD008163, 2007.

Shrivastava, M., Fast, J., Easter, R., Gustafson Jr., W. I., Zaveri, R. A., Jimenez, J. L., Saide, P., and Hodzic, A.: Modeling organic aerosols in a megacity: comparison of simple and complex representations of the volatility basis set approach, Atmos. Chem. Phys., 11, 6639–6662, doi:10.5194/acp-11-6639-2011, 2011.

Shrivastava, M., Zelenyuk, A., Imre, D., Easter, R., Beranek, J., Zaveri, R. A., and Fast, J.: Implications of low volatility SOA and gas-phase fragmentation reactions on SOA loadings and their spatial and temporal evolution in the atmosphere, J. Geophys. Res. Atmos., 118, 3328–3342, doi:10.1002/jgrd.50160, 2013.

Skamarock, W. C., Klemp, J. B., Dudhia, J., Gill, D. O., Barker, D. M., Wang, W., and Powers, J. G.: A description of the advanced research WRF version 3, NCAR Tech. Note, NCAR/TN-475+STR, Natl. Cent. Atmos. Res., Boulder, Colo, 2008.

Spracklen, D. V., Jimenez, J. L., Carslaw, K. S., Worsnop, D. R., Evans, M. J., Mann, G. W., Zhang, Q., Canagaratna, M. R., Allan, J., Coe, H., McFiggans, G., Rap, A., and Forster, P.: Aerosol mass spectrometer constraint on the global secondary organic aerosol budget, Atmos. Chem. Phys., 11, 12109–12136, doi:10.5194/acp-11-12109-2011, 2011.

Streets, D. G., Bond, T. C., Carmichael, G. R., Fernandes, S. D., Fu, Q., He, D., Klimont, Z., Nelson, S. M., Tsai, N. Y., Wang, M. Q., Woo, J.-H., and Yarber, K. F.: An inventory of

Title Page

Abstract	Introduction
Conclusions	References
Tables	Figures

|◀ | ▶|

◀ | ▶

Back | Close

Full Screen / Esc

Printer-friendly Version

Interactive Discussion

gaseous and primary aerosol emissions in Asia in the year 2000, J. Geophys. Res., 108, 8809, doi:10.1029/2002JD003093, 2003.

Takami, A., Miyoshi, T., Shimono, A., and Hatakeyama, S.: Chemical composition of fine aerosol measured by AMS at Fukue Island, Japan, during APEX period, Atmos. Environ., 39, 4913–4924, 2005.

Takami, A., Miyoshi, T., Shimono, A., Kaneyasu, N., Kato, S., Kajii, Y., and Hatakeyama, S.: Transport of anthropogenic aerosols from Asia and subsequent chemical transformation, J. Geophys. Res., 112, D22S31, doi:10.1029/2006JD008120, 2007.

Takegawa, N., Miyazaki, Y., Kondo, Y., Komazaki, Y., Miyakawa, T., Jimenez, J. L., Jayne, J. T., Worsnop, D. R., Allan, J., and Weber, R. J.: Characterization of an Aerodyne aerosol mass spectrometer (AMS): intercomparison with other aerosol instruments, Aerosol Sci. Tech., 39, 760–770, 2005.

Takegawa, N., Miyakawa, T., Kondo, Y., Blake, D. R., Kanaya, Y., Koike, M., Fukuda, M., Komazaki, Y., Miyazaki, Y., Shimono, A., and Takeuchi, T.: Evolution of submicron organic aerosol in polluted air exported from Tokyo, Geophys. Res. Lett., 33, L15814, doi:10.1029/2006GL025815, 2006a.

Takegawa, N., Miyakawa, T., Kondo, Y., Jimenez, J. L., Zhang, Q., Worsnop, D. R., and Fukuda, M.: Seasonal and diurnal variations of submicron organic aerosols in Tokyo observed using the Aerodyne aerosol mass spectrometer, J. Geophys. Res., 111, D11206, doi:10.1029/2005JD006515, 2006b.

Tang, Y., Carmichael, G. R., Uno, I., Woo, J.-H., Kurata, G., Lefer, B., Shetter, R. E., Huang, H., Anderson, B. E., Avery, M. A., Clarke, A. D., and Blake, D. R.: Impacts of aerosols and clouds on photolysis frequencies and photochemistry during TRACE-P: 2. Three-dimensional study using a regional chemical transport model, J. Geophys. Res., 108, 8822, doi:10.1029/2002JD003100, 2003.

Tang, Y., Carmichael, G. R., Seinfeld, J. H., Dabdub, D., Weber, R. J., Huebert, B., Clarke, A. D., Guazzotti, S. A., Sodeman, D. A., Prather, K. A., Uno, I., Woo, J.-H., Yienger, J. J., Streets, D. G., Quinn, P. K., Johnson, J. E., Song, C.-H., Grassian, V. H., Sandu, A., Talbot, R. W., and Dibb, J. E.: Three-dimensional simulations of inorganic aerosol distributions in east Asia during spring 2001, J. Geophys. Res., 109, D19S23, doi:10.1029/2003JD004201, 2004.

Title Page

Abstract | Introduction

Conclusions | References

Tables | Figures

|◀ | ▶|

◀ | ▶

Back | Close

Full Screen / Esc

Printer-friendly Version

Interactive Discussion

Tao, J., Shen, Z., Zhu, C., Yue, J., Cao, J., Liu, S., Zhu, L., and Zhang, R.: Seasonal variations and chemical characteristics of sub-micrometer particles (PM_1) in Guangzhou, China, Atmos. Res., 118, 222–231, 2012.

Tsigaridis, K. and Kanakidou, M.: Global modelling of secondary organic aerosol in the troposphere: a sensitivity analysis, Atmos. Chem. Phys., 3, 1849–1869, doi:10.5194/acp-3-1849-2003, 2003.

Tsigaridis, K. and Kanakidou, M.: Secondary organic aerosol importance in the future atmosphere, Atmos. Environ., 41, 4682–4692, 2007.

Tsigaridis, K., Lathière, J., Kanakidou, M., and Hauglustaine, D. A.: Naturally driven variability in the global secondary organic aerosol over a decade, Atmos. Chem. Phys., 5, 1891–1904, doi:10.5194/acp-5-1891-2005, 2005.

Tsigaridis, K., Krol, M., Dentener, F. J., Balkanski, Y., Lathière, J., Metzger, S., Hauglustaine, D. A., and Kanakidou, M.: Change in global aerosol composition since preindustrial times, Atmos. Chem. Phys., 6, 5143–5162, doi:10.5194/acp-6-5143-2006, 2006.

Tsimpidi, A. P., Karydis, V. A., Zavala, M., Lei, W., Molina, L., Ulbrich, I. M., Jimenez, J. L., and Pandis, S. N.: Evaluation of the volatility basis-set approach for the simulation of organic aerosol formation in the Mexico City metropolitan area, Atmos. Chem. Phys., 10, 525–546, doi:10.5194/acp-10-525-2010, 2010.

Tsimpidi, A. P., Karydis, V. A., Zavala, M., Lei, W., Bei, N., Molina, L., and Pandis, S. N.: Sources and production of organic aerosol in Mexico City: insights from the combination of a chemical transport model (PMCAMx-2008) and measurements during MILAGRO, Atmos. Chem. Phys., 11, 5153–5168, doi:10.5194/acp-11-5153-2011, 2011.

Turpin, B. J. and Lim, H. J.: Species contributions to $PM_{2.5}$ mass concentrations: revisiting common assumptions for estimating organic mass, Aerosol Sci. Tech., 35, 602– 610, 2001.

Utembe, S. R., Cooke, M. C., Archibald, A. T., Shallcross, D. E., Derwent, R. G., and Jenkin, M. E.: Simulating secondary organic aerosol in a 3-D Lagrangian chemistry transport model using the reduced Common Representative Intermediates mechanism (CRI v2-R5), Atmos. Environ., 45, 1604–1614, 2011.

van der Werf, G. R., Randerson, J. T., Giglio, L., Collatz, G. J., Mu, M., Kasibhatla, P. S., Morton, D. C., DeFries, R. S., Jin, Y., and van Leeuwen, T. T.: Global fire emissions and the contribution of deforestation, savanna, forest, agricultural, and peat fires (1997–2009), Atmos. Chem. Phys., 10, 11707–11735, doi:10.5194/acp-10-11707-2010, 2010.

Title Page

Abstract | Introduction

Conclusions | References

Tables | Figures

|◄ | ►|

◄ | ►

Back | Close

Full Screen / Esc

Printer-friendly Version

Interactive Discussion

Wesely, M. L.: Parameterization of surface resistances to gaseous dry deposition in regional-scale numerical models, Atmos. Environ., 23, 1293–1304, 1989.

Wexler, A. S., Lurmann, F. W., and Seinfeld, J. H.: Modelling urban and regional aerosols, Part I: Model development, Atmos. Environ., 28, 531–546, 1994.

Xiao, R., Takegawa, N., Zheng, M., Kondo, Y., Miyazaki, Y., Miyakawa, T., Hu, M., Shao, M., Zeng, L., Gong, Y., Lu, K., Deng, Z., Zhao, Y., and Zhang, Y. H.: Characterization and source apportionment of submicron aerosol with aerosol mass spectrometer during the PRIDE-PRD 2006 campaign, Atmos. Chem. Phys., 11, 6911–6929, doi:10.5194/acp-11-6911-2011, 2011.

Zaveri, R. A. and Peters, L. K.: A new lumped structure photochemical mechanism for large-scale applications, J. Geophys. Res., 104, 30387–30415, doi:10.1029/1999JD900876, 1999.

Zaveri, R. A., Easter, R. C., and Wexler, A. S.: A new method for multicomponent activity co-efficients of electrolytes in aqueous atmospheric aerosols, J. Geophys. Res., 110, D02201, doi:10.1029/2004JD004681, 2005a.

Zaveri, R. A., Easter, R. C., and Peters, L. K.: A computationally efficient Multicom-ponent Equilibrium Solver for Aerosols (MESA), J. Geophys. Res., 110, D24203, doi:10.1029/2004JD005618, 2005b.

Zaveri, R. A., Easter, R. C., Fast, J. D., and Peters, L. K.: Model for Simulat-ing Aerosol Interactions and Chemistry (MOSAIC), J. Geophys. Res., 113, D13204, doi:10.1029/2007JD008782, 2008.

Zhang, Q., Alfarra, M. R., Worsnop, D. R., Allan, J. D., Coe, H., Canagaratna, M. R., and Jimenez, J. L.: Deconvolution and quantification of hydrocarbon-like and oxygenated organic aerosols based on aerosol mass spectrometry, Environ. Sci. Technol., 39, 4938–4952, 2005.

Zhang, Q., Jimenez, J. L., Canagaratna, M. R., Allan, J. D., Coe, H., Ulbrich, I., Alfarra, M. R., Takami, A., Middlebrook, A. M., Sun, Y. L., Dzepina, K., Dunlea, E., Docherty, K., De-Carlo, P. F., Salcedo, D., Onasch, T., Jayne, J. T., Miyoshi, T., Shimono, A., Hatakeyama, S., Takegawa, N., Kondo, Y., Schneider, J., Drewnick, F., Borrmann, S., Weimer, S., Demerjian, K., Williams, P., Bower, K., Bahreini, R., Cottrell, L., Griffin, R. J., Rautiainen, J., Sun, J. Y., and Zhang, Y., M.: Ubiquity and dominance of oxygenated species in organic aerosols in anthropogenically influenced Northern Hemisphere midlatitudes, Geophys. Res. Lett., 34, L13801, doi:10.1029/2007GL029979, 2007.

Title Page

Abstract | Introduction

Conclusions | References

Tables | Figures

|◀ | ▶|

◀ | ▶

Back | Close

Full Screen / Esc

Printer-friendly Version

Interactive Discussion

Zhang, Q., Streets, D. G., Carmichael, G. R., He, K. B., Huo, H., Kannari, A., Klimont, Z., Park, I. S., Reddy, S., Fu, J. S., Chen, D., Duan, L., Lei, Y., Wang, L. T., and Yao, Z. L.: Asian emissions in 2006 for the NASA INTEX-B mission, Atmos. Chem. Phys., 9, 5131– 5153, 2009,

http://www.atmos-chem-phys.net/9/5131/2009/.

Zhang, Q. J., Beekmann, M., Drewnick, F., Freutel, F., Schneider, J., Crippa, M., Prevot, A. S. H., Baltensperger, U., Poulain, L., Wiedensohler, A., Sciare, J., Gros, V., Borbon, A., Colomb, A., Michoud, V., Doussin, J.-F., Denier van der Gon, H. A. C., Haeffelin, M., Dupont, J.-C., Siour, G., Petetin, H., Bessagnet, B., Pandis, S. N., Hodzic, A., Sanchez, O., Honoré, C., and Perrussel, O.: Formation of organic aerosol in the Paris region during the MEGAPOLI summer campaign: evaluation of the volatility-basis-set approach within the CHIMERE model, Atmos. Chem. Phys., 13, 5767–5790, doi:10.5194/acp-13-5767-2013, 2013.

VBS OA Simulation in East Asia

H. Matsui et al.

Title Page

Abstract	Introduction
Conclusions	References
Tables	Figures

|◄ | ►|

◄ | ►

Back | Close

Full Screen / Esc

Printer-friendly Version

Interactive Discussion

Table 1. Abbreviations for organic vapors and aerosols used in this study.

Abbreviation	Definition	Explanation
OA	Organic aerosol	–
POA	Primary OA	Primary emission or formed from SIVOCs
SOA	Secondary OA	Sum of OPOA, BSOA, and ASOA
VOCs	Volatile organic compounds	Primary emission
SIVOCs	Semi-volatile and intermediate volatility organic compounds	Primary emission (primary SIVOCs) or secondary production from primary SIVOCs (oxygenated SIVOCs)
OVOCs	Oxygenated volatile organic compounds	Oxidation products of VOCs
HOA	Hydrocarbon-like OA	Obtained by AMS
OOA	Oxygenated OA	Obtained by AMS
OPOA	Oxygenated POA	OA formed from SIVOCs
BSOA	Biogenic SOA	OA formed from biogenic OVOCs
ASOA	Anthropogenic SOA	OA formed from anthropogenic OVOCs (including biomass burning sources)

Table 2. Meteorological and chemical process options used in this study.

Atmospheric Process	Model Option
Longwave radiation	RRTM
Shortwave radiation	Goddard
Surface layer	Monin-Obukhov
Land surface	Noah
Boundary layer	YSU
Cumulus clouds	Kain-Fritsch
Cloud microphysics	Morrison
Gas-phase chemistry	SAPRC99
Aerosol nucleation	Binary nucleation
Aerosol condensation	MOSAIC
Aerosol coagulation	COAGSOLV
Aqueous-phase chemistry	Fahey and Pandis
Photolysis	Fast-J

Table 3. Summary of the VBS schemes developed in this study and original WRF-chem/MOSAIC model.

Item/Process	This Study	Shrivastava et al. (2011)
Gas-phase chemistry	SAPRC99	SAPRC99
VBS volatility species	9 for POA and primary SIVOCs	9 for POA and primary SIVOCs
	8 for OPOA and oxygenated SIVOCs	8 for OPOA and oxygenated SIVOCs
	4 for ASOA, BSOA, and OVOCs	4 for ASOA, BSOA, and OVOCs
Oxidation species	VOCs, SIVOCs, and OVOCs	VOCs and SIVOCs
OVOCs formation	NO_x-dependent 4-product fit (Tsimpidi et al., 2010)	NO_x-dependent 4-product fit (Tsimpidi et al., 2010)
Gas-particle partitioning	Bulk equilibrium (Schell et al., 2001)	Bulk equilibrium (Donahue et al., 2006)
OA distribution to each size bin	Koo et al. (2003)	Koo et al. (2003)
Number of size bin	8 (40–10 000 nm)	4 (40–10 000 nm)
Number of variables in VBS	122	380
	Gas-phase: 53	Gas-phase: 76
	Bulk aerosol: 53	Size-resolved aerosol: 304
	Size-resolved aerosol: 16	
	(interstitial aerosol, in-cloud aerosol)	
Dry deposition	On	On
Aerosol activation	On	Off
Wet deposition	On	Off

Table 4. List of model simulations.

Simulation	Aging coefficient ($cm^3\,molecule^{-1}\,s^{-1}$)	
	SIVOCs and anthropogenic OVOCs	Biogenic OVOCs
Aging-on	1×10^{-11}	1×10^{-11}
Aging-off	0	0
Aging-an	1×10^{-11}	0
Aging-bio	0	1×10^{-11}
Aging-0.25	2.5×10^{-12}	2.5×10^{-12}
Aging-4	4×10^{-11}	4×10^{-11}

Table 5. Statistics of concentrations of chemical species at the surface measurement sites.

Station	Period	Species	Units	Mean concentration			NMB (%) [b]	R [b]
				Observation	Calculation[a] (Aging-on)	Calculation[a] (Aging-off)		
Komaba	19 Jul–13 Aug 2003 (IMPACT-2)	O_3	ppbv	19.6	15.3	15.4	−22.3	0.63
		SOA	$\mu g\,m^{-3}$	4.36	3.45	1.03	−20.8	0.52
Kisai	25 Jul–14 Aug 2004 (IMPACT-L)	O_3	ppbv	26.4	20.6	20.7	−21.9	0.84
		SOA	$\mu g\,m^{-3}$	5.31	4.61	0.76	−13.1	0.70
Fukue	27 Mar–26 Apr 2009	SO_4	$\mu g\,m^{-3}$	9.31	8.29	8.27	−10.9	0.65
		OA	$\mu g\,m^{-3}$	6.02	6.75	0.71	12.2	0.34
		OA/SO_4	–	0.89	0.78	0.13	−11.9	0.28
Hedo	24 Mar–26 Apr 2009	SO_4	$\mu g\,m^{-3}$	2.36	4.20	4.24	78.0	0.34
		OA	$\mu g\,m^{-3}$	1.08	1.99	0.18	84.2	0.25
		OA/SO_4	–	0.58	0.42	0.058	−29.7	0.58

[a] Values are calculated for the periods when measurements are available.
[b] Statistics are calculated for the Aging-on simulation.

Table 6. Period-averaged organic aerosol mass concentration (μg m^{-3}) in the boundary layer (~ 1 km) over the outer domain.

Simulation	POA	OPOA	ASOA	BSOA	Total OA
Aging-on	0.236	0.369	0.333	0.346	1.284
Aging-off	0.164	0.000	0.023	0.048	0.236
Aging-an	0.229	0.357	0.313	0.111	1.004
Aging-bio	0.196	0.000	0.038	0.241	0.474
Aging-0.25	0.188	0.056	0.106	0.132	0.483
Aging-4	0.275	1.223	0.661	0.654	2.813
Aging-on (an off)[a]	0.047	0.035	0.007	0.075	0.165
Aging-off (an off)[a]	0.040	0.000	0.001	0.018	0.059

[a] Simulations without anthropogenic emissions (with biomass burning, biogenic, and volcanic emissions).
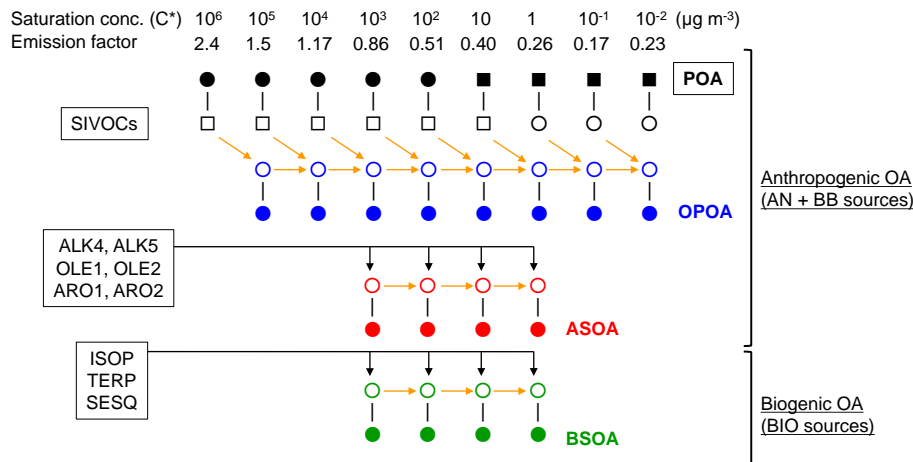
Fig. 1. Summary of the volatility basis-set approach used in this study. Circles and squares show individual gas-phase (open) and aerosol-phase (closed) surrogate species. Squares denote primary emission species. AN, BB, and BIO denote anthropogenic, biomass burning, and biogenic sources, respectively. The oxidation processes shown by black arrows are calculated with the coefficients given by Tsimipidi et al. (2010). The oxidation process shown by orange arrows are calculated assuming OH oxidation with the rate coefficient of $1 \times 10^{-11}\,\mathrm{cm}^{-3}\,\mathrm{molecule}^{-1}\,\mathrm{s}^{-1}$.
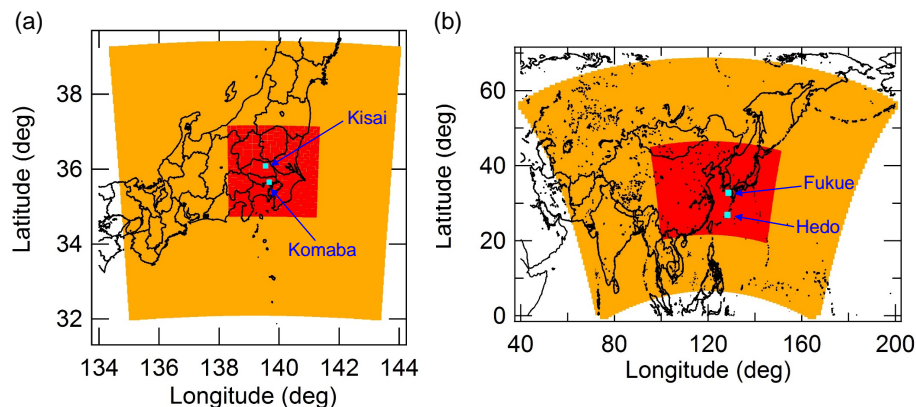
Fig. 2. Simulation domains **(a)** in and around Tokyo during the IMPACT campaign and **(b)** over East Asia during the A-FORCE campaign. **(a)** Simulations were conducted for 17 July to 15 August 2003 (IMPACT-2) and for 23 July to 15 August 2004 (IMPACT-L) with horizontal resolutions of 27 km (outer domain, orange) and 9 km (inner domain, red). Light blue squares show the locations of measurement stations at Komaba ($35.66°$ N, $139.67°$ E) and Kisai ($36.08°$ N, $139.55°$ E). **(b)** Simulations were conducted for 21 March to 26 April 2009 with horizontal resolutions of 180 km (outer domain, orange) and 60 km (inner domain, red). Light blue squares show the locations of measurement stations at Fukue ($32.75°$ N, $128.68°$ E) and Kisai ($26.87°$ N, $128.25°$ E).
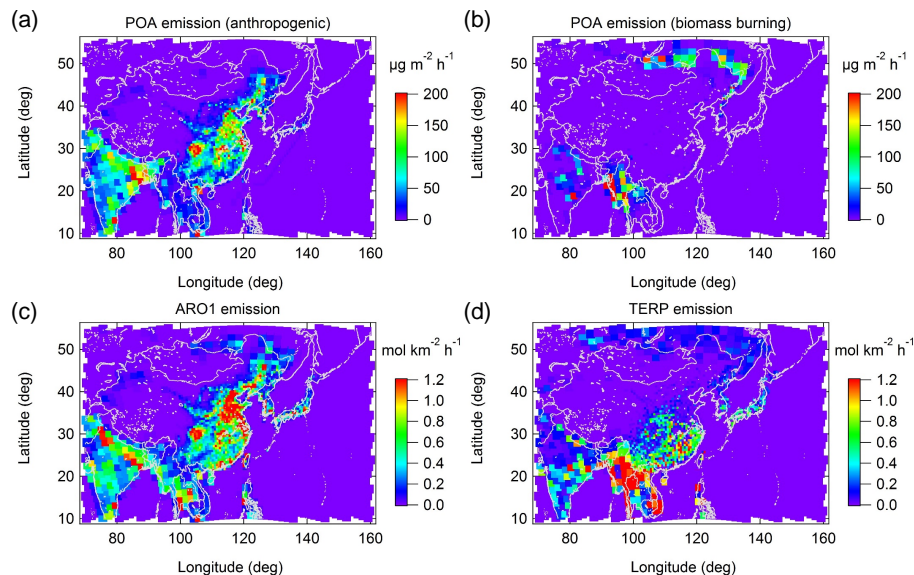
Fig. 3. Period-averaged (24 March–26 April 2009) emissions for **(a)** POA from anthropogenic sources (fossil fuel and biofuel combustion), **(b)** POA from biomass burning sources, **(c)** ARO1 (aromatics), and **(d)** TERP (monoterpenes). We used the anthropogenic and volcanic emission inventories of Streets et al. (2003), daily biomass burning emissions of the Global Fire Emissions Database version 3 (GFED3) (van der Werf et al., 2010), and on-line biogenic emissions of the Model of Emissions of Gases and Aerosols from Nature version 2 (MEGAN2) (Guenther et al., 2006).
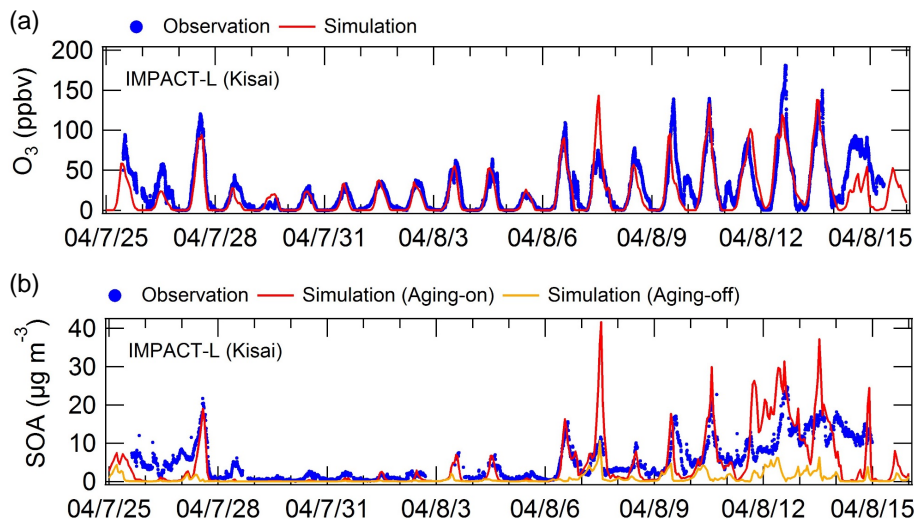
Fig. 4. Time series of observed and simulated **(a)** O$_3$ volume mixing ratio and **(b)** SOA mass concentrations at Kisai during the IMPACT-L campaign. SOA values were simulated with and without aging.

Fig. 5. Correlation of SOA mass concentrations with O_3 volume mixing ratio **(a)** at Komaba during the IMPACT-2 campaign and **(b)** at Kisai during the IMPACT-L campaign. Solid lines show fitting slopes ($y = ax$) for observation (blue) and simulations with (red) and without (orange) aging processes of organic vapors.
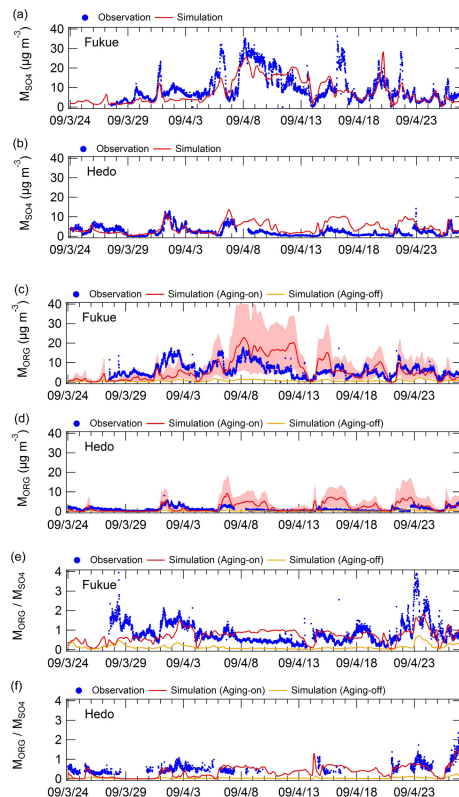
Fig. 6. Time series of **(a, b)** sulfate mass concentrations, **(c, d)** organic aerosol mass concentrations, and **(e, f)** organic to sulfate mass concentration ratios at Fukue and Hedo, respectively. Red shading in panels **(c)** and **(d)** shows the range of organic aerosol mass concentrations with the aging coefficient between 4×10^{-11} cm^3 molecule^{-1} s^{-1} (4 times the base case) and 2.5×10^{-12} cm^3 molecule^{-1} s^{-1} (1/4 times the base case). The periods when observed sulfate mass concentrations were less than 1 µg m^{-3} are not shown for measurements (blue points) in panels **(e)** and **(f)**.
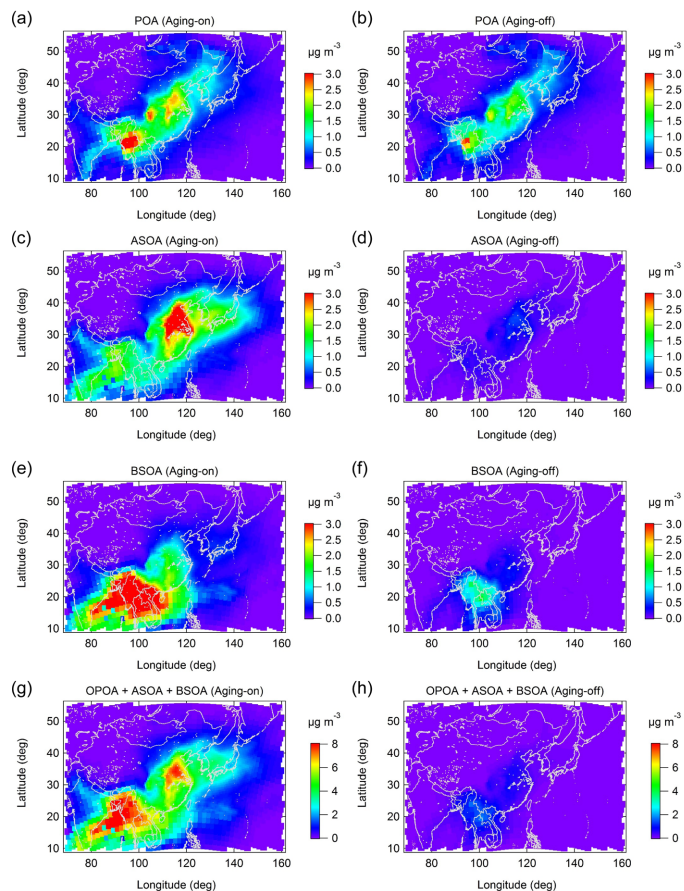
Fig. 7. Period-averaged (24 March–26 April 2009) simulated mass concentrations of POA **(a, b)**, ASOA **(c, d)**, BSOA **(e, f)**, and total SOA (sum of OPOA, ASOA, and BSOA) **(g, h)** at an altitude of about 1 km (sigma level of 0.895). Left panels **(a, c, e, g)** are runs with aging, and right panels **(b, d, f, h)** are runs without aging.
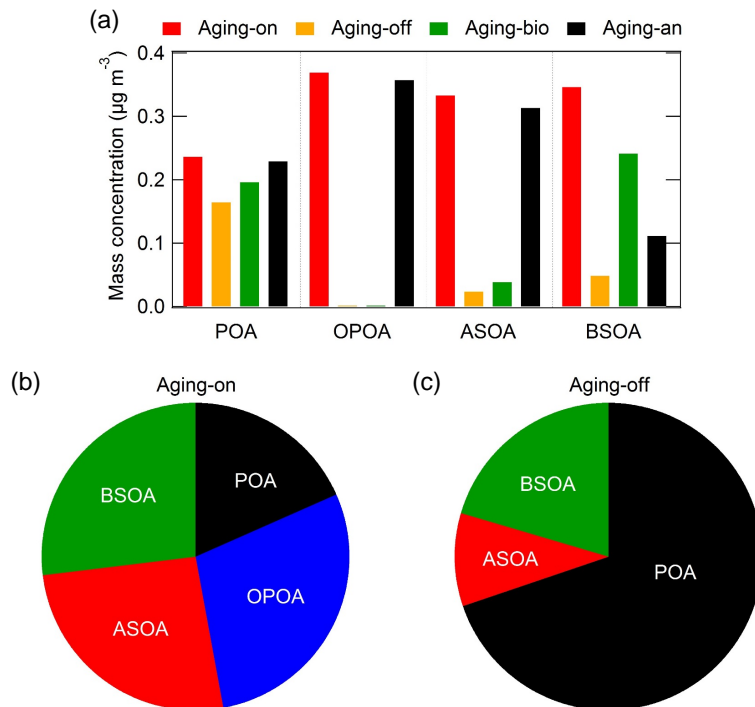
Title Page

Abstract | Introduction

Conclusions | References

Tables | Figures

⏮ | ⏭

◀ | ▶

Back | Close

Full Screen / Esc

Printer-friendly Version

Interactive Discussion

Fig. 8. Period-averaged (24 March–26 April 2009) mass concentrations of POA, OPOA, ASOA, and BSOA at an altitude of about 1 km (sigma level of 0.895) over the outer domain for Aging-on, Aging-off, Aging-bio, and Aging-an simulations **(a)**. Period-averaged fraction of POA, OPOA, ASOA, and BSOA to total OA mass concentrations at an altitude of about 1 km (sigma level of 0.895) over the outer domain for simulations with **(b)** or without **(c)** aging.
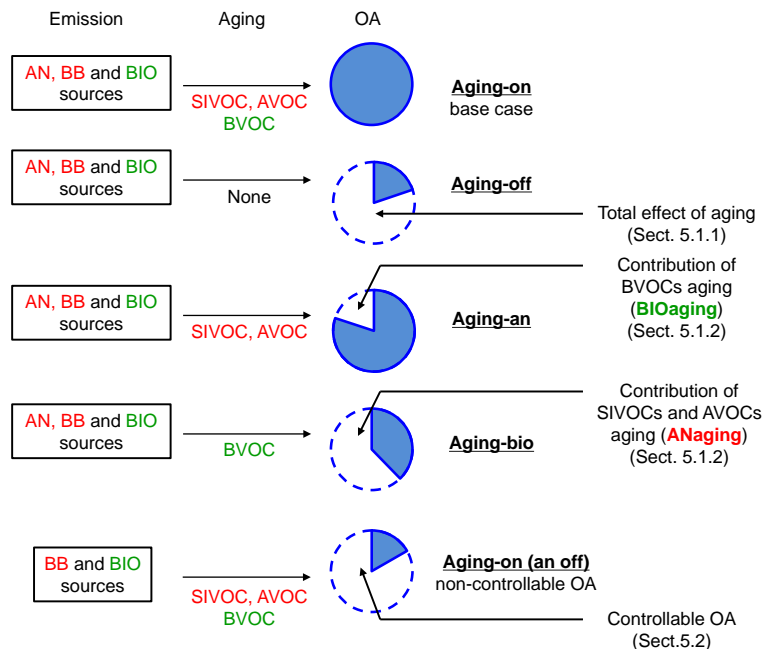
Fig. 9. Diagram of sensitivity simulations conducted in Sect. 5. OA contributions estimated from individual simulations are shown. AVOC and BVOC denote anthropogenic and biogenic OVOCs, respectively.

Title Page

Abstract | Introduction

Conclusions | References

Tables | Figures

|◄ | ►|

◄ | ►

Back | Close

Full Screen / Esc

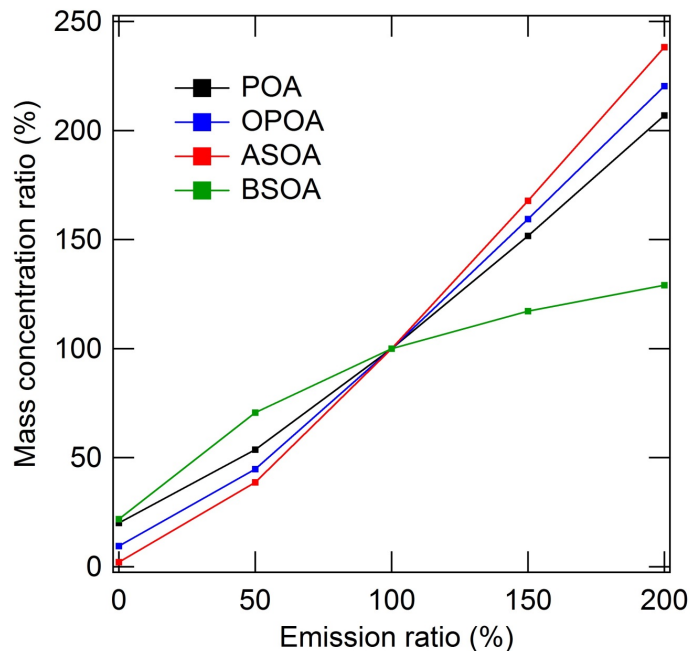Printer-friendly Version

Interactive Discussion

Fig. 10. Sensitivity of POA, OPOA, ASOA, and BSOA mass concentrations to changes in anthropogenic emissions (CO, NO_x, SO_2, VOCs, SIVOCs, POA and black carbon) at an altitude of about 1 km (sigma level of 0.895) over the outer domain. Mass concentrations and anthropogenic emissions in the sensitivity simulations are normalized by those in the base case simulation.

Title Page

Abstract | Introduction

Conclusions | References

Tables | Figures

|◄ | ►|

◄ | ►

Back | Close

Full Screen / Esc
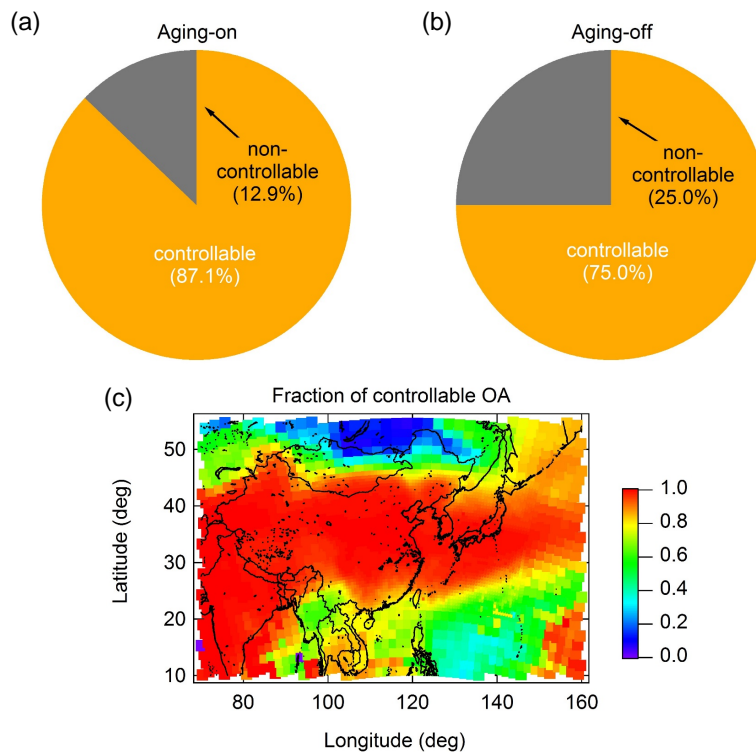
Printer-friendly Version

Interactive Discussion

Fig. 11. Period-averaged (24 March–26 April 2009) fraction of controllable and non-controllable OA mass concentrations at an altitude of about 1 km (sigma level of 0.895) over the outer domain for simulations with **(a)** or without **(b)** aging. Period-averaged (24 March–26 April 2009) fraction of controllable OA at an altitude of about 1 km (sigma level of 0.895) over the outer domain for the simulation with aging **(c)**.

Title Page

Abstract | Introduction

Conclusions | References

Tables | Figures

|◀ | ▶|

◀ | ▶

Back | Close

Full Screen / Esc

Printer-friendly Version

Interactive Discussion